# BOREHOLE GEOLOGY AND HYDROTHERMAL MINERALISATION OF WELL OW-35, OLKARIA EAST GEOTHERMAL FIELD, CENTRAL KENYA RIFT VALLEY

**Michael Mwania, Samuel Munyiri and Emily Okech**
Kenya Electricity Generating Company Ltd. – KenGen
P.O. Box 785-20117
Naivasha
KENYA
*mmwania@kengen.co.ke; smunyiri@kengen.co.ke; eokech@kengen.co.ke*

## ABSTRACT

Well OW-35 is a production well located in the Olkaria East field within the Greater Olkaria geothermal system. This is a vertical well drilled to a depth of 2988 m below ground level with a maximum allowable deviation of 5°. The aim of drilling this well was to enhance the steam supply for the upcoming Olkaria I units IV & V power plants and to confirm the resource extent to the southwest of the East production field. Analyses of rock cuttings were carried out from the top to the bottom of the well. Three major feed zones were observed at 800-1200, 1600-1800 and 2800-2988 m, and other minor feed zones were noted between 2400 and 2700 m. The lithological units encountered were predominantly comprised of pyroclastics, rhyolites, trachytes, breccias, basalts, tuffs, and intrusions. The surface rocks consist of unconsolidated rock formations, which have not been subjected to significant geothermal alteration. The alteration distribution in the well shows high temperatures defined by the first appearance of epidote at 678 m, indicating temperatures >240°C. Other high-temperature alteration minerals include actinolite and wollastonite observed at 1624 and 2064 m, respectively. Clay analysis showed distinct mineralisation sequences ranging through smectite - MLC (smectite-chlorite) – chlorite - illite. Fluid inclusion analysis was carried out for pre-selected depths at 644-646 and 1722-1724 m to determine the homogenization temperatures ($T_h$) at which the fluids were trapped. The fluid analysis reflects the highest temperature of 235°C for the former depth and 310°C for the latter.

## 1. INTRODUCTION

Well OW-35 is a vertical well drilled in the Olkaria East production field (EPF) and is situated in the Olkaria volcanic complex in the central sector of the Kenya Rift (Figure 1). It is defined by the UTM coordinates at 199824.82 m Easting and 9902209.95 m Northing with an elevation of 1960.66 m. The well was aimed at exploiting the resource in the East production field to supply steam to upcoming Olkaria 1 units IV and V. Well OW-35 was drilled to a depth of 2988 m with the surface, anchor and production casings installed at 50, 290 and 827 m, respectively.
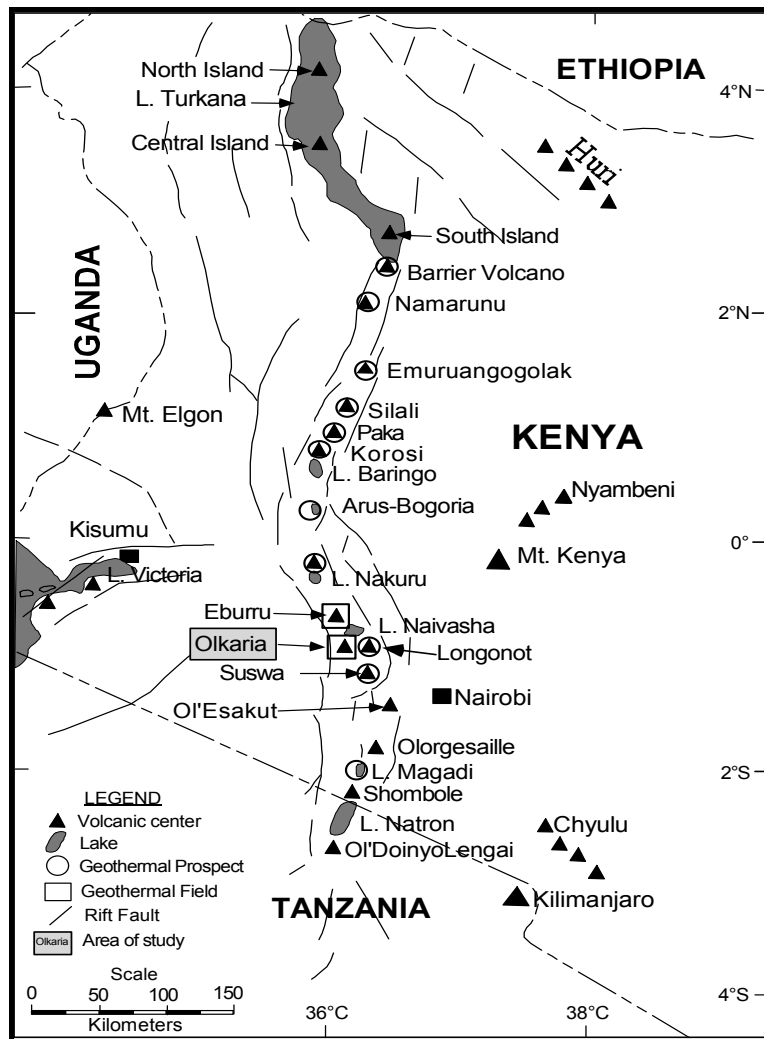
## 1.1 Objective of study

The main aim of this study was to determine the geothermal conditions in the Olkaria East production field by examining the lithology, hydrothermal mineralisation, the sequence of mineral deposition in veins and vesicles, the locations of aquifers, and the temperature conditions of the reservoir in well OW-35.

The current study elucidates the prevailing conditions of the well to ascertain the viability of the well to supply steam to the upcoming Olkaria I units IV and V power plant. However, there is need for further intense study on a larger scale to correlate the surrounding wells so as to determine hydrothermal mineralisation and possibly the factors controlling the mineralisation patterns, thus understanding the geothermal system within the East production field.

This report is a requirement stipulated by the United Nations University Geo-thermal Training Programme (UNU-GTP) to manifest the participation in the three month *Course on Geothermal Technology* and the six month *Advanced Training in Borehole Geology* that took place at KenGen in Naivasha from 16th April, 2012 to 1st February, 2013.



FIGURE 1: Map of the Kenya rift showing the location of Olkaria geothermal field and other Quaternary volcanoes along the rift axis (Lagat, 2004)

## 1.2 Climate and vegetation

The area is classified as having a semi-humid to semi-arid warm temperate climate. Rainfall over the greater part of this area is favourable for plant growth, with regular periods of precipitation. Rainfall is concentrated in the months of March to May and October to December, although it is generally expected that the hottest part of the year is from January to March with the wettest month being in April. Average annual rainfall is 500-700 mm (Braun, 1980).

The general vegetation is dominated by stunted thorn shrubs, bushes and vast expanses of savannah grassland. The physiography of the area is generally rugged and characterized by numerous hills among which is included Olkaria Hill. The drainage pattern is actually uneven and apparently controlled by the nature of the topography with observable incised valley channels draining the general area toward areas of low altitude (Clarke et al., 1990).

## 2. REGIONAL GEOLOGY

The East African Rift (EARS) is an active continental rift zone in east Africa that appears to be a developing divergent tectonic plate boundary where rift tectonics accompanied by intense volcanism has taken place from the Tertiary to recent (Figure 2), (Chorowicz, 2005).

According to Baker et al. (1971, 1972), Baker and Wohlenberg (1971), Smith (1994), Smith and Mosley (1993) and Lagat (2004), the African Rift is structurally controlled and was formed due to tectonic activities involving faulting and fracturing at the collisional zones between the Archean Tanzania craton and the Proterozoic orogenic belts. The EARS is composed of a series of several thousand kilometres long (40-80 km wide) aligned successions of adjacent individual tectonic basins (rift valleys), separated from each other by relative shoals and generally bordered by uplifted shoulders (Hardarson, 2012).

The tectonic activities led to the formation of two upper mantle upwellings and subsequent pressure releases manifested as plumes (Figure 3). The plumes indicate the presence of at least two distinct mantle plumes beneath the East African Rift System (EARS), providing separate dynamic support for the Ethiopian and East African plateaus, respectively (Rogers et al., 2000). These plumes are known as the Kenya and Afar mantle plumes and are illustrated in Figure 3. These plumes are characterized by basaltic extrusions, i.e. the Kenyan and Ethiopian flood basalts. These basalts have been analysed for Sr,
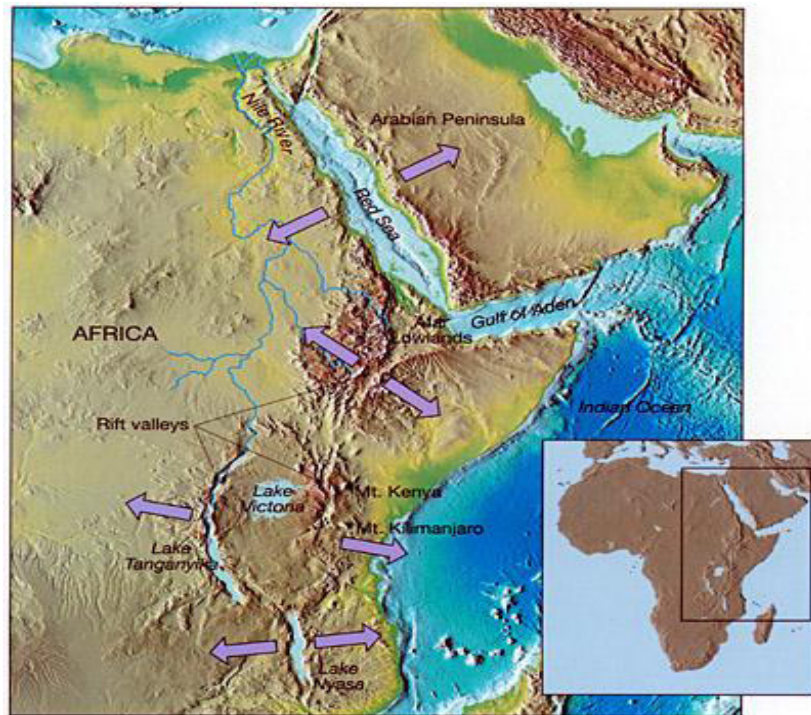


FIGURE 2: Plate showing the EARS divergent tectonic plate boundary (from Chorowicz, 2005)
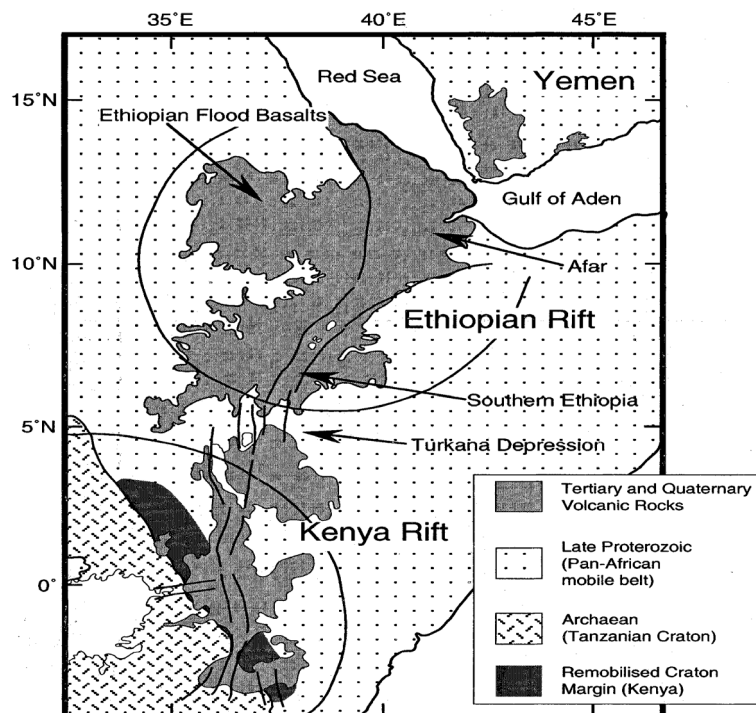


FIGURE 3: Sketch map of the Kenya and Ethiopia rifts, showing the distribution of Tertiary-recent volcanism, Cratonic and mobile belt and the reworked craton margin as mapped out in Kenya; the curved solid lines denote the extent of the Ethiopian and East African plateaus and the faint lines mark the strike of the major border faults of the main rift valleys (Rogers et al., 2000)

Nd and Pb isotopes. The isotopic characteristics of the Afar plume suggest a deep origin in a gas-unsaturated part of the mantle, while the Kenyan plume may have a shallow origin, as inferred from seismic tomography (Simiyu and Keller, 1997, Simiyu et al., 1995). Lagat (2004) implied that extensive volcanic eruptions occurred in the Miocene period. The magmatic activity was accompanied by domal uplift of about 300 m on the crest of the erupted phonolites.

The Pliocene trachytic ignimbrite eruptions from the central area of the rift formed the Mau and Kinangop tuffs. Later, further faulting resulted in the development of a graben structure, and fissure eruptions, mostly of trachytes, basalts, basaltic trachyandesites and trachyandesites, took place. Plateau rocks later filled the graben structure and were then faulted to form the high angle normal faults within the rift floor. The resultant fractures served as good conduits for Quaternary felsic and mafic volcanics. Some of these formations were observed in the drill cuttings of well OW-35.

Simiyu and Keller (1997) estimated the crustal thickness beneath the graben valley to vary in depth from 3 to 5 km. Geophysical (seismic) data indicate the overall thickness of the most intense volcanic activity at the central sector of the rift to be about 5 km (Baker et al., 1972).

## 3. GEOLOGY OF THE GREATER OLKARIA VOLCANIC COMPLEX

The Greater Olkaria volcanic complex is located in the central sector of the Kenya Dome and has an estimated crustal thickness of 30-35 km beneath it (Mechie et al., 1997). According to Clarke et al. (1990), the age of the complex is estimated to be between 22-20 ka BP. There are six historic stages that led to its current state. This report will briefly describe these occurrences, which are also summarized in Figure 4.

*Stage 1:* The initial pre-caldera trachytic magmatism caused the sequence exposing the Olkaria Trachyte formation (Ot) and Maiella pumice formation (Mp). The pumice and trachytes are widespread and may have erupted from vents within the volcanic complex. The trachyte lavas are exposed mainly in gullies and ridges in the southwest part of the complex (MacDonald et al., 2008; Marshall et al., 2009).

*Stage 2:* The trachyte eruptions were followed by a caldera collapse, forming a depression 11 × 7.5 km across (Clarke et al., 1990). The collapse is evidenced by a well-
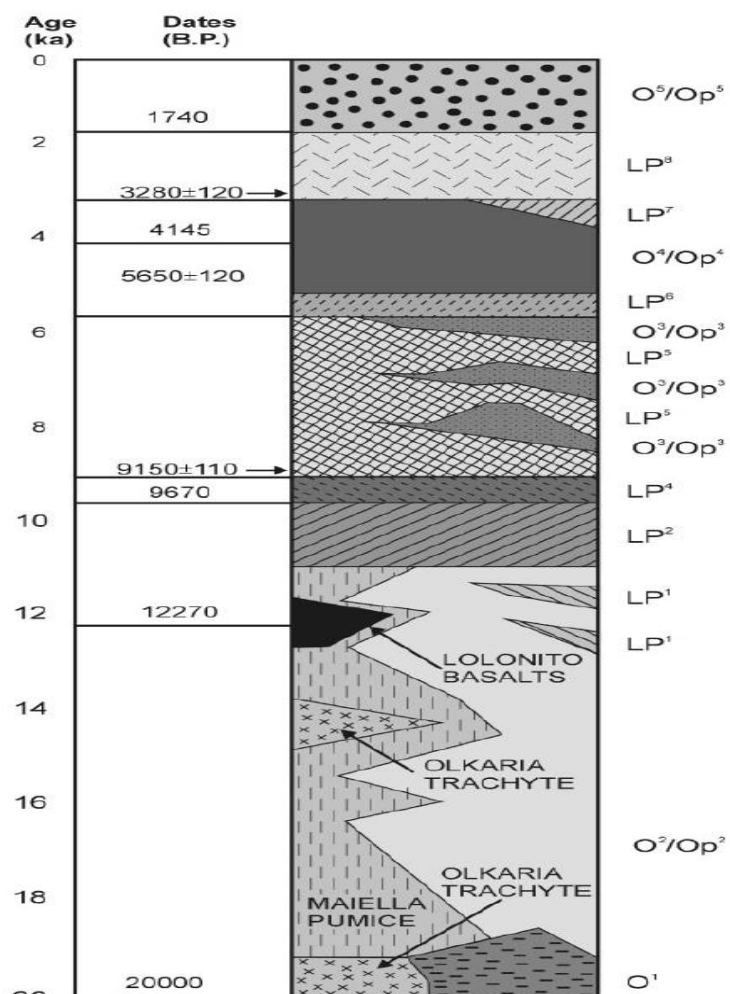
FIGURE 4: Stratigraphic column for the Olkaria complex (Marshall et al., 2009)

developed ring structure, the presence of a ring of rhyolite domes, pyroclastic deposits around this structure, apparent resurgent activity within the ring structure and the distribution of fumaroles around the collapsed caldera. This collapse has been associated with the eruption of welded pyroclastic rocks of the Ol Njorowa pantellerite formation ($O_1$).

The lower comendite formation ($O_2$) represents the post-caldera activity linked to the eruption of peralkaline rhyolitic lavas and pyroclastic rocks ($Op_2$). The predominant dome-building phase of the middle comendite member ($O_3$) followed, with the eruption of thick surge deposits ($Op_3$), comendite member ($O_4$); the most recent activity is the eruption of very thick flows of comendite ($O_5$) from a north-south fissure zone. The youngest flow dated to $180\pm50$ BP (Clarke et al., 1990).

*Stage 3*: Magmatic eruptions of the lower comendite member of the Olkaria comendite formation preceded the caldera's collapse. It is represented by rhyolitic lavas and pyroclastics, dated at $>9150 \pm 110$ BP using the $^{14}C$ method. The Olkaria volcanic complex does not have a clearly visible caldera. However, its association with the ring of volcanic domes in the east, south, and southwest has been used to infer the presence of a buried caldera (Naylor, 1972; Virkir, 1980; Clarke et al., 1990; Mungania, 1992).

*Stage 4*: The middle comendite member extrusion period was a period of ring dome formation, comprised mainly of rhyolitic lavas and the eruption of thick pyroclastic deposits, which happened between $>9150 \pm 110$ and $>3280 \pm 120$ BP.

*Stage 5:* During this stage, there was a notable resurgence of the caldera floor and the formation of thick lava flows that resulted in the upper comendite member.

*Stage 6:* The last flow signified eruptions of very thick lava flows of comendite from a north–south fissure system. The youngest lava flow, Ololbutot comendite, was dated $180 \pm 50$ BP (Clarke et al., 1990).

According to Omenda (2000), the sub-surface geology of the Greater Olkaria volcanic complex can be divided into six main rock types: the Proterozoic basement formation, pre-Mau volcanics, Mau tuffs, plateau trachytes, Olkaria basalt and upper Olkaria volcanics. This has been deduced from the analysis of rock cuttings from wells drilled in Olkaria. The wells do not intercept any of the basement formation due to depths greater than 3000 m.

The basement system is overlain by the pre-Mau volcanics consisting of basalts and ignimbrites which vary in thickness. The Mau tuffs overlie the pre-Mau volcanics, which are common in the area west of Olkaria Hill but are absent in the east due to an east-dipping high-angle fault that passes through Olkaria Hill (Omenda, 1994, 1998).

## 3.1 Structural geology

The structure of the rift valley, in particular the major marginal and rift faults, the system of grid faulting and the rift floor undoubtedly have substantial effect on the geothermal fluid flow systems of the area. In general, faults are considered to have two effects on fluid flow. They may facilitate flow by providing channels of high permeability, or they may provide barriers to flow by offsetting zones of relatively high permeability (Chorowicz, 2005).

Within the Rift Valley, the main direction of faulting is along the axis of the rift, and this has a significant effect on the flows across the rift. It is apparent from the high hydraulic gradients which developed across the rift escarpments that the major faults act as zones of low permeability.

In the Greater Olkaria geothermal area (GOGA), there is evidence of near vertical step-faulting. These fault scarps are often well preserved and marker horizons can be progressively traced on lower slopes. It is notable that the greater portion of the fault blocks plunge southwards. There are other faults striking northwest, linking the parallel rift basins to the main extensional zone (Wheeler and Karson, 1994).

Among the many faults is the ENE-WSW Olkaria fault. This is one of the major faults running through the Olkaria geothermal area. Omenda (1998) presumed the fault to be an older and rejuvenated structure. The fault manifests itself on the surface as a linear zone of intense geothermal manifestations and highly altered grounds, about 50-100 m in width. Fumaroles in this area are at boiling point with sulphur and silica deposits observed on the surface. This fault has a surface displacement of about 5 m with a down-throw to the north (Omenda, 1998).
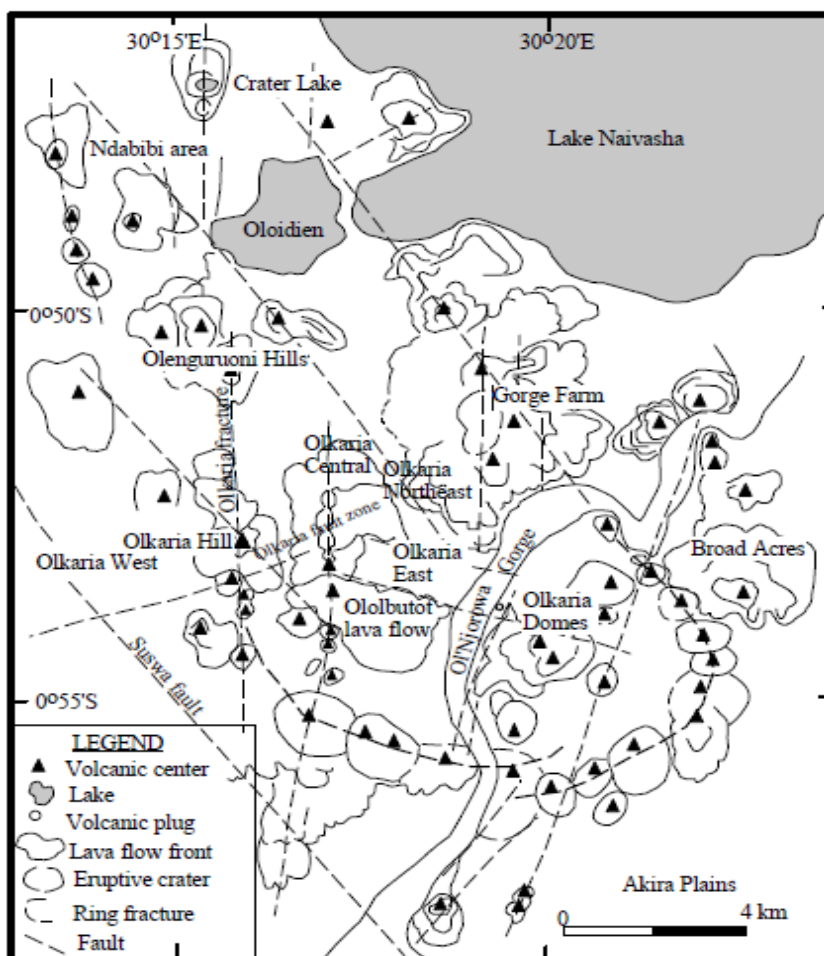
The Gorge Farm fault runs NW-SE from Lake Naivasha and extends to the Olkaria Domes area (Lagat, 2004). This fault is envisaged to be a major recharge zone for GOGA.

A system of fissures and faults running E-W is believed to control the bulk of fluid movement and permeability properties of the reservoir rocks in the Olkaria West Field and Domes areas (Odongo, 1993). As observed in Figure 5, a major fault runs from Olkaria Hill eastwards to end up below the younger lava flow at the east of Ol Njorowa gorge.

The N-S structural controls are demonstrated by the ease of movement of geothermal fluids from one monitoring well to another. A tracer injection study was carried out by Karingithi (1996) where well OW-R3 was injected with 4,000 litres of cold lake water stained with



FIGURE 5:  Main structures in the Greater Olkaria geothermal (Lagat, 2004)

500 kg of an organic dye, Sodium Fluorescein, and pumped continuously for an hour. It was noted that the rate of fluid flow per given time was higher in the structurally interconnected paths.

In this study, nine wells were monitored (OW-34, OW-32, OW-30, OW-29, OW-28, OW-26, OW-25, OW-24, and OW-10) for tracer and thermal breakthrough. This test did not include well OW-35 as the well had not yet been drilled. The results are shown in Table 1.

TABLE 1:  Well parameters showing tracer travel time

| Well no. | Radial distance from OW-R3 (m) | No. of travel days for the tracer | Rate of tracer travel (m/day) |
|---|---|---|---|
| OW-34 | 780 | 40 | 19.5 |
| OW-32 | 340 | 30 | 11.3 |
| OW-30 | 840 | 70 | 12.6 |
| OW-29 | 1160 | 103 | 11.6 |
| OW-26 | 1500 | 120 | 12.5 |
| OW-25 | 1120 | 60 | 9.33 |
| OW-24 | 1110 | 131 | 8.47 |
| OW-28 | 700 | 124 | 5.65 |
| OW-10 | 1400 | 125 | 11.2 |

Karingithi (1996) had several interesting observations, listed below:

- Permeability allowed the stained fluid to be traced in all the monitoring wells.
- The tracer travel times differed greatly, probably due to structural conditions and the radial distance from OW-R3.
- He noted that there must be a hydrogeological/tectonic barrier between wells OW-R3, OW-32 and OW-34.
- However, the travel time was much less between well OW-R3 and other wells, i.e. OW-30, OW-29 and OW-25.  This was due to high fluid flux caused by a flow path in the NW-SE orientation.  This is further projected by the NW-SE structural orientations in Olkaria.

## 3.2  Hydrogeology

This section describes the hydrological characteristics of systems replenishing target aquifers in the vast Olkaria project area.

The hydrogeology of an area is controlled by the type of litho-stratigraphic units, the degree of alteration and structural features such as joints and faults that characterize an area.  These will have an effect on both the primary and secondary porosity of rocks.

### 3.2.1  Groundwater resources

The potential of an area in terms of its groundwater reservoirs is largely dependent on the existing recharge to these underground systems.  In the present area, studies have indicated a continuous recharge mechanism into these systems through outflows from Lake Naivasha, a fact supported by its fresh character though there is no surface manifestation of outflow (Saggerson, 1963).

The groundwater occurrence in Olkaria is controlled by complex tectonics and geological formations that characterize the area.  It is notable that most of the lithostratigraphic contacts and fissure zones covering the rift floor constitute the most important aquifers in the area as they are highly permeable.

Phase II of the optimization studies carried out in Olkaria indicated that the geothermal system is recharged in two different scenarios:  there are deeper aquifers, indicated by isotope data studies, showing recharge to be from the northern parts of the Great Rift System, while shallow aquifers consist of cold influence and are mainly recharged by the fissure system, i.e. the Ololbutot fracture zone and the Gorge Farm fault.  They source their water from the western Rift escarpment (Gylfadóttir et al., 2011).

The high gradients caused by the relative location of Lake Naivasha in relation to other areas within the Rift floor account for the outflow of groundwater from the lake to the south as well as some infinitesimal outflows to the north. Structural features such as faults often optimize storage, transmissivity and recharge, with the most significant of these occurring in places that are adjacent to or within a surface drainage system (Driscoll, 1986).

### 3.3 Geophysical setting

The geophysical prospects are positive in the Olkaria geothermal field and indicate zones of low resistivity (<20 Ωm) anomalies at depths of 1000 m a.s.l. These low-resistivity zones are good indicators of the heat source (Simiyu, 1999).

According to Gylfadóttir et al. (2011), geophysical data probes that were analysed indicate an underlying magma chamber in the Greater Olkaria geothermal system, which is assumed to be lying very deep beneath the surface. The magma chamber has three main outlets that intrude to shallower depths of 6-8 km below ground level. These intrusions manifest themselves to the surface as hills, calderas, etc. These presumed heat bodies, which may consist of partially molten magma, lie beneath Olkaria Hill (supplying the West field), in the northeast beneath the Gorge Farm volcanic centre (supplying the Northeast field), and in the Domes area (Figure 6).

Heat upflow is controlled by linear structures in NE-SW and NW-SE directions. The near surface difference in resistivity is caused by contrasts in the subsurface geology. From geophysical data combined with alteration mineralogy and reservoir data collected in drilled wells, it is evident that the low-resistivity areas lie at 1000 m a.s.l. Drilled wells show that the low-resistivity areas have formation temperatures of about 240°C. However, areas that correspond to shallow recharge from the western escarpment faulting will portray a characteristic cold-flow scenario (Lichoro, 2009).
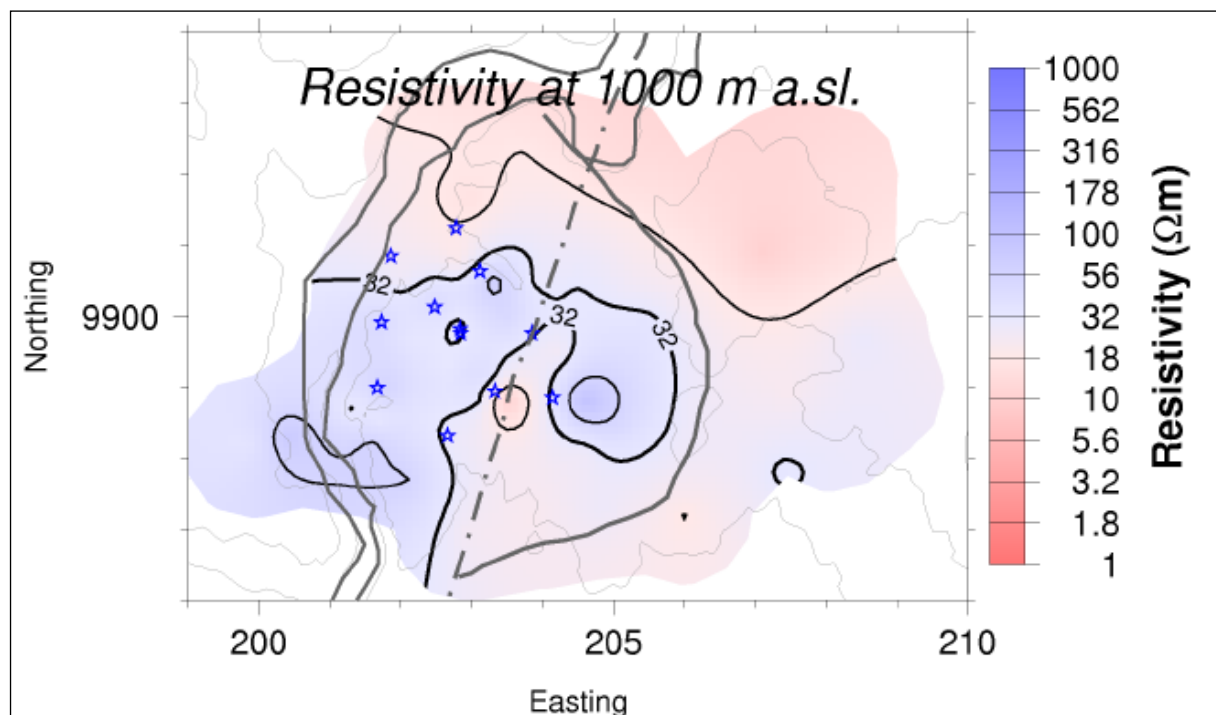


FIGURE 6: Resistivity data for the Greater Olkaria area

**3.4 Geochemistry**

There is a great difference in the fluid chemistry of the Olkaria East, Olkaria West and Olkaria Northeast fields (Lagat, 2004). The West field discharges bicarbonate-rich fluid (10,000 ppm). The fluid has notably low Cl- concentrations (50-200 ppm). This means it is not in proximity to any heat source. On the other hand, the Northeast field has much lower bicarbonate content waters, with levels decreasing to <1000 ppm and Cl- levels rising to 400-600 ppm.

Comparatively, the Olkaria East field wells discharge fluids with bicarbonate concentrations of <200 ppm, similar to the West field. The Cl- concentrations are relatively low compared to Olkaria Northeast concentrations with deep reservoir Cl- concentrations of 200-350 ppm. Olkaria Central wells have deep reservoir Cl- concentrations of 200-300 ppm. These wells produce waters with relatively high reservoir $CO_2$ concentrations, similar to those of the Olkaria West field wells. Olkaria Domes wells discharge mixed sodium-bicarbonate-chloride-sulphate type water with low mean chloride concentrations of 181.5-269.9 ppm (Lagat, 2004).

Well OW-35 was observed to exhibit high Cl- levels, unlike other wells in the Olkaria East field discussed above (Figure 7). The Cl- - $SO_4^{2-}$ – $HCO_3^-$ levels are plotted in the ternary diagram below. From the analysed fluid samples, it was noted that the Cl- levels range between 500-2300 ppm (90% Cl- concentration). This signifies mature waters that are in close communication with the reservoir. This fact is further proven by the conceptual model, which indicates the existence of an upflow zone around this well.
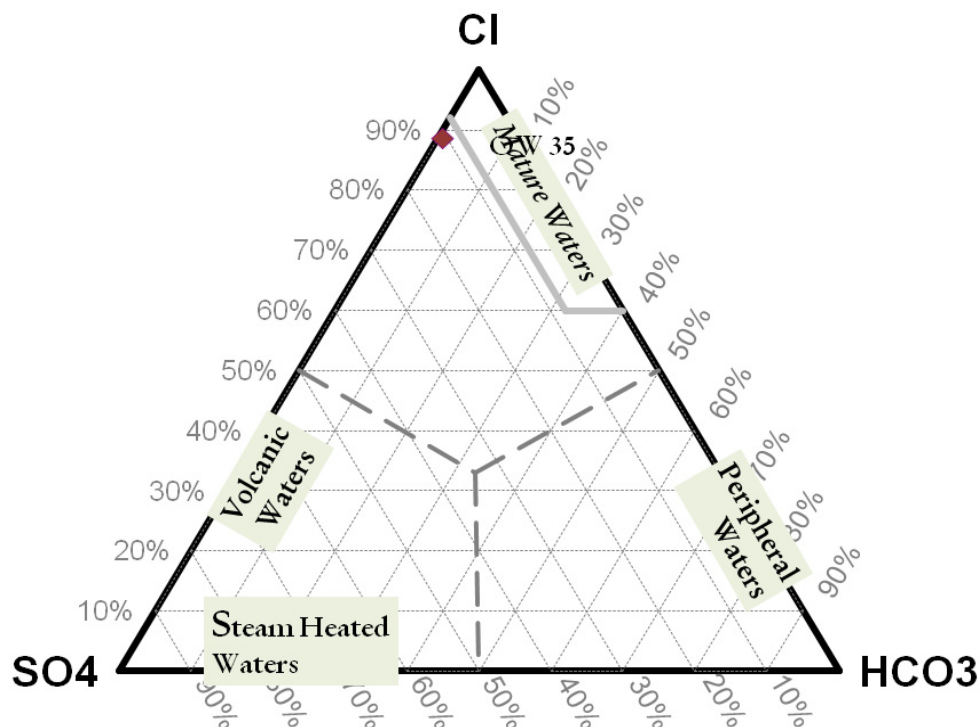


FIGURE 7:  Ternary diagram showing the position of
well OW-35 with chloride rich waters

The Olkaria conceptual model (Figure 8) shows the upflow zones in the Greater Olkaria geothermal area. The East production field forms one of the upflow zones, a phenomenon that contributes to good productivity of the wells in that area. The chemistry of well OW-35 also indicates a composition of high Cl- compared to other wells in the same region. This implies that it could be closer to the heat source or in direct communication with the heat source, probably through the vast fissure system.
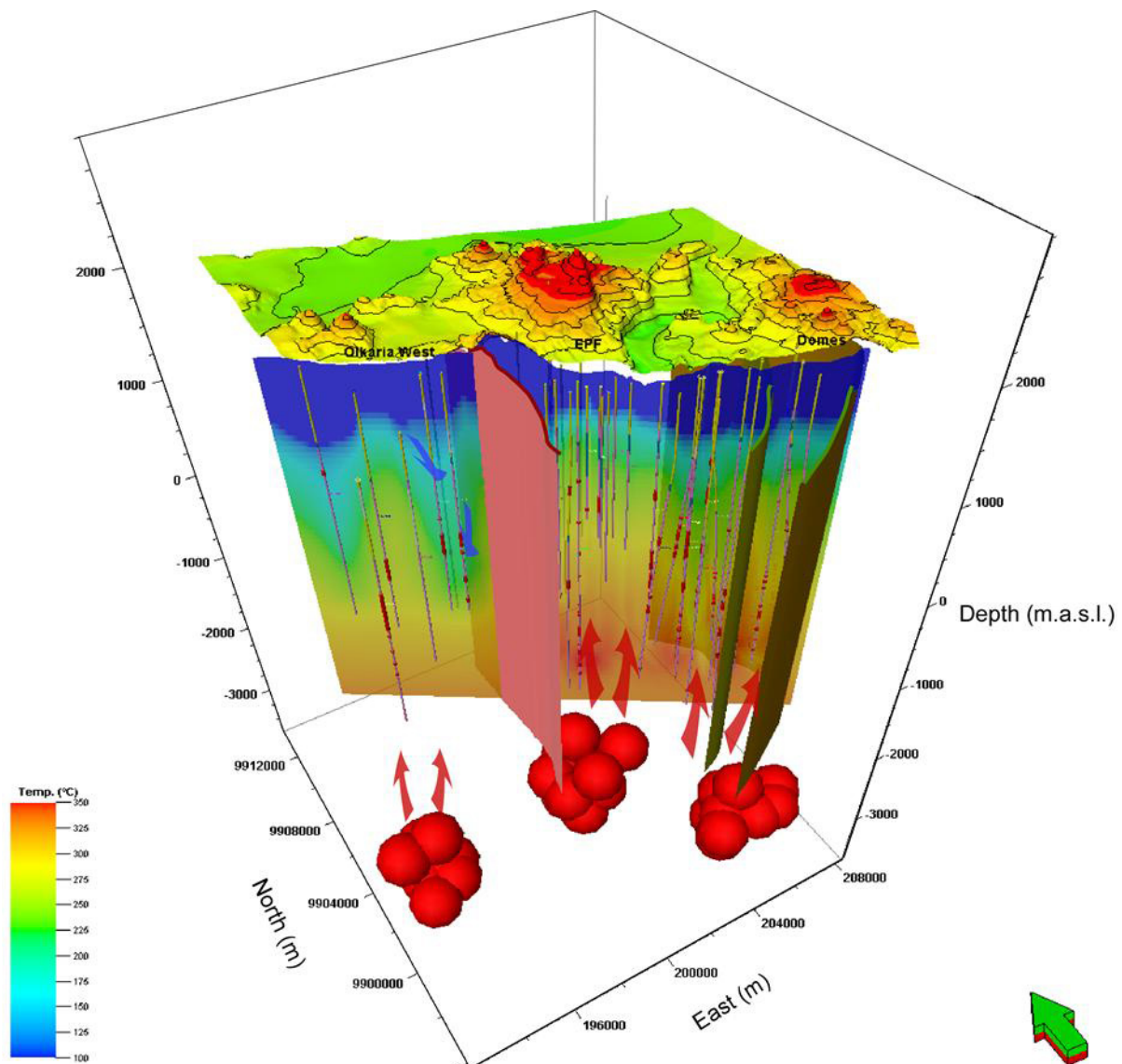
FIGURE 8:  A schematic of the revised conceptual model of the Greater Olkaria geothermal system
based on the data review and interpretation; the green arrow in bottom left is directed to
north; the top layer shows the topography, and the Ololbutot fault is shown along
with parts of the ring structure (Gylfadóttir et al., 2011)

## 4.  BOREHOLE GEOLOGY

### 4.1  Drilling Process

Well OW-35 was spudded on 4th October, 2010 at 0012 hrs and completed on 18th November, 2010.  It
was drilled to a total depth of 2988 m to supply additional steam to the proposed Olkaria I units IV and
V power stations.  The maximum allowable deviation was 5°.  It is one of the production wells drilled
in the Olkaria East high-temperature geothermal field.  The well is located about 400 m northeast of
the Olkaria I power station as shown in Figure 9, the well coordinates being 199824.815 m Easting
and 9902209.951 m Northing at an elevation of 1960.657 m a.s.l.

FIGURE 9:  Location of well OW-35; both blue and green paths indicate directions of wells with the blue lines representing the drilled wells while green lines represent wells that have not been drilled

Drilling was carried out by the Great Wall Drilling Company (GWDC) from China under the special supervision of Kenya Electricity Generating Company (KenGen), and was carried out in four stages, starting on 4th October, 2010, ending on 18th November, 2010, 45 days in total, as shown in Figure 10.

*Phase 1:* The well was spudded at 00:12 hrs on Monday 4th October, 2010 with drill rig GW-120, drilling with a 26" inch drill bit, and circulating the hole with mud down to 50 m. Running in the 20" surface casing took place at 14:50, on the spud date. About 17.61 tonnes of



FIGURE 10:  Drilling progress of well OW-35

cement were used for the cementing job. The blow-out preventer (BOP) was also installed on 6th October after the cementing job was completed. Circulation losses were experienced at several depths and are considered feed zones in the well.

*Phase 2:* The rig crew commenced drilling using a 17½" bit from 7th October to 9th October, 2010. The anchor casing was placed down to 290 m. Subsequently, the 13⅜" anchor casing was installed and about 45.4 tonnes of cement were used during cementing and took three days to set.

*Phase 3*: From 12th to 18th October, 2010, drilling resumed using a 12¼" bit down to 827 m using aerated water and foam with good circulation returns except between 798 and 802 m where circulation losses were experienced. The 9⅝" production casing was installed. Cementing was done using about 65.3 tonnes of cement.

*Phase 4*: This involved drilling using an 8½" bit down to the bottom of the well (2988 m) with aerated water and foam with major circulation losses experienced at 676-680, 772-784, 1386-1396, 1678-1686, 1750-1752, 1872-1876, 2216-2222, 2308-2318, 2444-2464, 2478-2488, 2564-2570, 2604-2614, 2634-2648, 2668-2674, 2688-2692, 2706-2712, 2730-2740, 2748-2758, 2764-2768, 2786-2790, 2834-2842, 2920-2926 and 2976-2980 m. A final depth of 2988 m was reached on 18th November, 2010 and the 7" slotted liners were successfully installed to the final depth.

Well completion tests were then conducted for two days, showing an increase in temperature with depth and the master valve was installed. An overview of all the drilling stages and casing point details are shown in Table 2.

TABLE 2: Drilling and casing depths in well OW-35

| Drill rig | Stage | Depth (m) | | Casing type | |
|---|---|---|---|---|---|
| | | From | To | (") | (Particulars) |
| GW-120 | Phase 1 | 0 | 50 | 20 | Surface casing |
| | Phase 2 | 50 | 290 | 13⅜ | Anchor casing |
| | Phase 3 | 290 | 827 | 9⅝ | Production casing |
| | Phase 4 | 827 | 2988 | 7 | Slotted liners |

**4.1.1 Sampling and analysis**

Rock cuttings were collected at 2 to 4 m intervals, depending on the returns recovery rate. Over a few metres interval, partial to total loss of returns to the surface was experienced; hence no samples were collected. Drilling fluid returns were collected at 50 m intervals to observe the chemistry profile throughout the well bore. Inflow and outflow temperature logs were also taken at 20 m intervals from 827 m, where the production zone began. No cores were collected since the geology of the area is understood and coring is considered rather expensive unless otherwise requested by the rig geologist. Therefore, the lithological descriptions are entirely based on drill cuttings.

Drill cuttings were first analysed at the rig site to determine: colour(s) of the cuttings, rock type(s), grain size, rock fabrics, alteration mineralogy and intensity, vein and vesicle infillings and lithological boundaries. They were later taken to the core shed for cleaning and drying. After drying, some cuttings, spaced at 50 m intervals, were taken to the XRD section for clay analysis. The clay analyses were carried out using **PowDLL** and **DiffracPlus EVA** softwares, the former used to convert the XRD **Shimadzu** data type to **Brucker** type, while the latter was used to evaluate the different clay types. Other samples were chosen as per the geologist's instructions for petrographic and fluid inclusion analysis.

In thin sections, confirmation of the rock types, alteration minerals and alteration mineral sequences were determined. For the fluid inclusion study, calcite and quartz crystals were carefully selected to determine the temperatures at which they were formed during crystallization (homogenization temperature, $T_h$).

The drill fluid samples were handed in to the Geochemistry Department for geochemical testing and analysis. Temperature logs are important to generally determine the formation temperature of the reservoir with depth and the location of feed zones.

## 4.2 Stratigraphy of well OW-35

Well OW-35 was logged by the rig geologist and daily geological reports consisting of the lithologic units were compiled. The geologist used a binocular microscope and, after well completion, the petrographic thin sections and XRD clay analysis data were used to confirm rock properties of the encountered lithostratigraphic succession. Later, a detailed stratigraphy was constructed down to a depth of 2988 m, as summarised in Figure 11. The rock types encountered were pyroclastics, trachytes, trachy-andesites, tuffs, rhyolites, basalts and, to a lesser extent, syenites as intrusions. Loss zones were also recorded as depths where circulation returns were not received on the surface during drilling. A brief description of each rock type is outlined hereafter, while the comprehensive descriptions are in Appendix I.

### 4.2.1 Pyroclastics

This stratum occurs at a depth of 0-50 m as greyish to brown unconsolidated material consisting of soil, glassy pumice, obsidian, lithic material and weathered fragments. From the binocular microscopy, traces of felsic minerals were observed. Yellowish sulphur deposition was also noted in the matrix from 16 to 30 m. Alteration minerals reported include minor calcite, chalcedony, pyrite and oxides from 38 m.

### 4.2.2 Rhyolite

Most of the non-comenditic rhyolite extrusions of the well were noted at shallow depths of 50 to 122 m, with a characteristic oxidation of most of the observed samples. Due to their extrusive nature, their grain size is aphanitic and they rarely have euhedral crystals due to the accelerated cooling. However, the matrix was observed to be of felsic composition. With deeper penetration, from 70 m, quartz phenocrysts were observed.

In the rock cuttings, the typical rhyolites were white, pink, and light to pale grey felsic to porphyritic rocks, usually containing visible quartz in deeper and less exposed parts. The pumiceous rhyolites were spongy, highly porous whitish to dirty grey rocks, usually able to float on water for a limited period. There were textural gradations from compact rhyolites to pumice.

Rhyolites also occurred at deeper depths of 982-992, 1018-1028, 2512-2540, 2548-2552 and 2902-2910 m.

An intrusion with rhyolitic composition was noted from 2206 to 2234 m, with a white colour, medium to coarse grained and composed of notable quartz crystals. It showed a moderate to high degree of alteration (see Figure 11).

### 4.2.3 Breccia and tuff

Breccia was noted at 124-130 m and occurred as fragmented and cemented material in a fine-grained matrix of anhedral habit. It appeared as yellow to greenish, non-crystalline and sub-angular fragments composed of chalcedony and minor clays (limonite). The stratum was highly oxidized, probably due to its fractured nature. Vein fillings were also noted in the sample, a further indication of fracturing. The breccia occurrence was rare, only noted at the shallow depth indicated above. Tuffs were thicker than breccias, underlying them to a depth of 238 m. They were yellow, green and grey, fine grained with occasional quartz crystals observed at greater depths from 210 m. The tuffs showed varying

degrees of oxidation and alteration. They were moderately to highly altered to green smectite. Chalcedony and fluorite were also noted in vesicles and fractured surfaces. They occurred interchangeably with other rock types throughout the well.
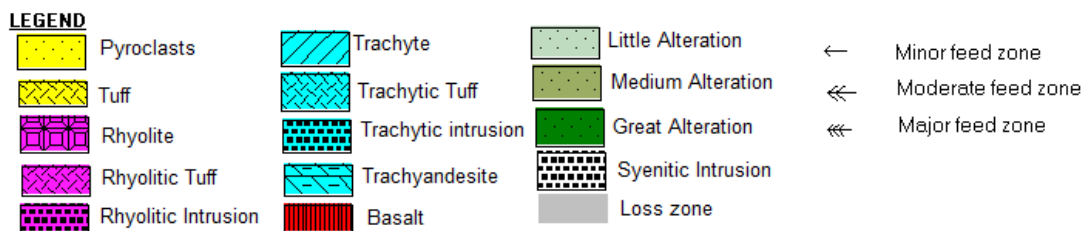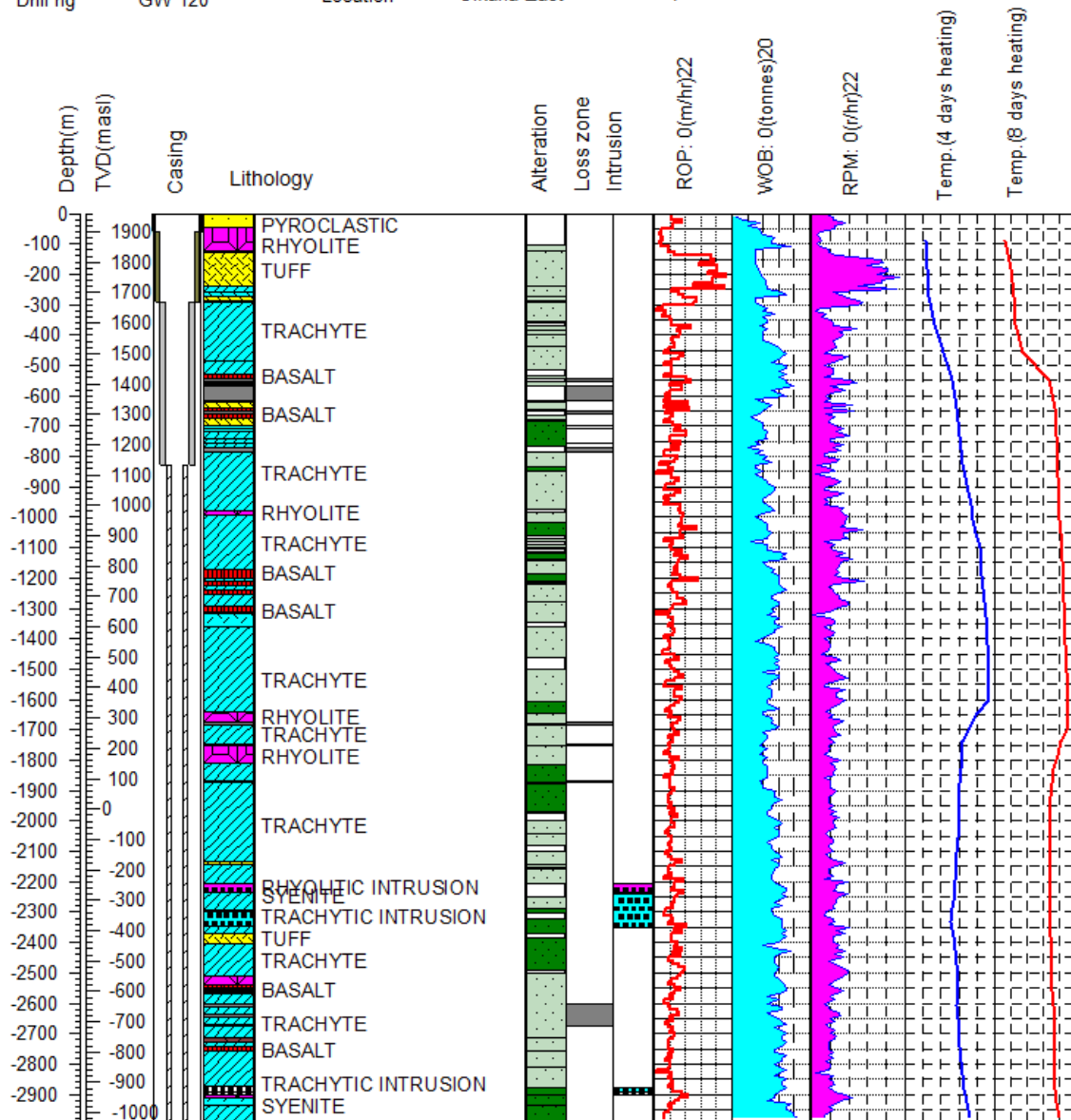


FIGURE 11: Shows various drilling lithological units, alteration intensity, feed zones, weight on bit (WOB), rate of penetration (ROP) and temperature logs for well OW-35

**Homogeneous tuff:** The thickest stratum was noted at 124-238 m. This showed quite an extensive and violent extrusion period that led to the deposition of the ash that consolidated to homogeneous tuff. Other deposits occur at 276-286, 430-434, 486-492, 554-556, 678-690, 2136-2142 and 2382-2404 m.

**Acidic tuff:** These occurred between 622 and 640 m, as dark grey, fine-grained lithic material with a characteristic silica-enriched composition. They are also known as rhyolitic tuffs. Rhyolite tuffs contain pumiceous, glassy fragments and small scoria with quartz, alkali feldspar, biotite, etc. The broken pumice is clear and isotropic, and very small particles commonly have crescentic, sickle-shaped, or biconcave outlines, showing that they were produced by the shattering of vesicular glass, sometimes described as ash-structure. The tiny glass fragments derived from broken pumice are called shards; the glass shards readily deform and flow when the deposits are sufficiently hot.

**Trachytic tuffs:** These were also popular among the tuffs, with various colours ranging from light grey, green and yellow, homogeneous and vesicular fragments, more being of trachytic composition in association with glassy to cryptocrystalline. Sanidine porphyrites are rarely seen in rock cuttings, but were observed at depths of 694-716, 1320-1360, 2374-2382 and 2912-2934 m.

### 4.2.4 Trachyte and trachy-andesite

Trachyte is the most dominant rock in the East production field, randomly alternating with rhyolite, tuffs and basalt. Trachyte was first identified at 240-260 m. Trachyte appears as grey, brown to yellow, fine- to medium-grained extrusive rock. Sanidine phenocrysts, which are characteristic of trachyte in Olkaria, were noted and ranged widely in size, the maximum measuring 5 mm (Lagat, 2004).

At shallower depths, the sanidines were minute, probably due to sudden cooling during the flow. Trachyte has a characteristic flow texture notable in most samples. Most crystals show preferred orientation aligned by the lava during the extrusion and crystallization phase.

A trachytic intrusion was observed at 2878 m with a thickness of about 14 m. It appeared as earth grey, massive, medium-grained and moderately altered rock. Sanidines were replaced by epidote and clays. As shown in Figure 11, trachyte also occurred at 294-380, 438-528, 566-570, 716-1172, 1200-1208, 1228-1238, 1258-1292, 1314-1318, 1362-1462, 2000-2134, 2144-2204, 2236-2366, 2408-2510, 2574-2712, 2728-2740 and 2758-2894 m.

Trachy-andesites are not common and were only noted from 262 to 272 m. They appeared as greyish and fine grained, with occasional quartz and abundant plagioclase laths.

### 4.2.5 Basalt

The first appearance of basalt was at 382 m. It appeared as dark grey with brown specs of ferromagnesian minerals, fine grained, massive, with characteristic plagioclase laths in thin sections. Pyroxenes and olivines were also noted at shallow depths where the basalt was less altered. At greater depths, most of the olivines were altered to clays and epidote. The typical greyish metallic lustre at the contact between the intrusion and the adjacent rocks was due to contact metamorphism (Clarke et al., 1990).

Other basaltic flows were noted between 530-542, 560-562, 618-620, 642-648, 1174-1198, 1210-1224, 1240-1256, 1296-1312, 2542-2546, 2554-2560, 2714-2726 and 2742-2756 m (see Figure 11).

**4.2.6 Syenite intrusion**

A syenite intrusion occurred as white, felsic, equigranular, medium-grained rock, which is feldspar and quartz rich, with notable aegerine-augite and arfvedsonite crystals seen in thin section. A syenite intrusion was observed at 2894-2900 m (see Figure 11).

**4.3 Aquifers/feed zones**

There were notable feed zones throughout the well bore, characterized by circulation losses, alteration mineralogy, fractured rocks, and lithostratigraphic contacts in the well logging profiles (Table 3). Major feed zones were restricted to the intervals 1550-1800 and 2900-2988 m, while minor feed zones were noted from 2400 to 2900 m.

Losses of circulation were noted at the following depths: 676-680, 772-784, 1386-1396, 1678-1686, 1750-1752, 1872-1876, 2216-2222, 2308-2318, 2444-2464, 2478-2488, 2564-2570, 2604-2614, 2634-2648, 2668-2674, 2688-2692, 2706-2712, 2730-2740, 2748-2758, 2764-2768, 2786-2790, 2834-2842, 2920-2926 and 2976-2980 m. Since the production casing was installed at 827 m, the first two loss zones were cased off.

Lithological contacts can also form good feed zones and are known to connect parallel aquifers, especially where drilling has taken place. There are trachyte-rhyolite contacts at 982, 992, 1018, 1028, 2206 and 2208 m. Trachyte-basalt contacts were noted at 1172, 1198, 1208, 1228, 1240 and 1296 m. Altered and fractured rocks also form good feed zones and were also noted throughout the well profiles. Figure 11 illustrates the interpreted permeable zones noted in well OW-35.

TABLE 3: Interpreted permeable zones/aquifers based on geological observations

| Depth (m) | Evidence from geological observations and drilling observations |
|---|---|
| 542 – 552 | Circulation losses |
| 570 – 616 | Circulation losses |
| 650 – 662 | Circulation losses |
| 696 – 698 | Circulation losses |
| 706 – 710 | Circulation losses |
| 754 – 756 | Circulation losses |
| 770 – 784 | Circulation losses |
| 980 – 982 | Contact between fractured trachyte and rhyolite |
| 1172 – 1174 | Contact between basalt and trachyte |
| 1238 – 1240 | Contact between basalt and trachyte |
| 1312 – 1314 | Contact between basalt and trachyte |
| 1676 – 1874 | Circulation losses |
| 2204 – 2206 | Contact between trachyte and rhyolitic intrusion |
| 2292 – 2294 | Contact between trachyte and syenite |
| 2548 – 2550 | Contact between basalt and rhyolite |
| 2564 – 2674 | Circulation losses |
| 2712 – 2726 | Primary porosity of scoria |
| 2772 – 2874 | Contact between trachyte and syenite |

**5. HYDROTHERMAL ALTERATION MINERALOGY**

Alteration in rocks refers to changes in the mineralogy of the rock due to changes in the prevailing conditions resulting in primary minerals being replaced by secondary minerals. Hydrothermal

alteration is a change in mineralogy as a result of the interaction of rock with hot water fluids, called "hydrothermal fluids" (Lagat, 2004). The fluids carry metals in solution, either from a nearby source, or from leaching out of some nearby rocks.

Factors influencing the distribution and kind of hydrothermal mineral assemblage include: permeability, composition of the host rock and the circulating fluids, temperature, pressure and duration of hydrothermal alteration. These factors are largely independent, but the effects of one or more of the factors can exert a dominant influence on the location and extent of hydrothermal alteration (Browne, 1978).

## 5.1 Alteration of primary minerals

In the Olkaria geothermal field, the rocks occurring at the surface include comendites, pumice fall and ash deposits. These are underlain by major rock types which include pyroclasts, trachyte, rhyolite, tuff and basalt with occasional intrusives at depth, predominantly syenites, rhyolites and granitic intrusions. Once these rocks interact with the circulating fluids and are subjected to changes in the prevailing conditions, the primary minerals are altered and replaced by secondary minerals.

The different alteration types that can be recognized in this well can be broadly grouped into two: the *supergene* and the *hypogene alterations,* apparently dependent on the environment or zones of the hydrothermal activity. In the near surface supergene environment, within a depth range of 0-480 m, the rocks are subjected to argillic alteration where low-temperature groundwater becomes acidic and the clay minerals are introduced, mainly smectite, zeolites and illite at presumed temperatures of <180°C. This is usually associated with the silicification type of alteration commonly known as "silica flooding", resulting from the deposition of amorphous/micro-crystalline silica, mainly chalcedony (Williams et al., 1985).

With more advanced temperatures, argillic alteration grades into phyllic alteration, often characterized by the occurrence of chlorite, illite, intermittent epidote and wairakite with sporadic wollastonite at temperatures of 200-270°C. This zone was observed to extend from 640 to 2150 m. In hypogene environments within a depth range of 2150-3000 m, the phyllic alteration advances to prophyllic alteration characterized by mineral assemblages of wairakite, quartz, epidote, chlorite, albite, illite, and prehnite at temperatures greater than 240°C. Notably, at high-temperature prophyllic alteration, amphiboles occur with actinolite being the most dominant mineral (at temperatures >280°C).

The susceptibility of the main primary minerals to hydrothermal alteration depends on Bowen's Reaction Series where the earlier formed minerals are the first to alter, whereas the later formed are the last to alter, with quartz mostly being unaffected (Thomas, 2010) (Figure 12). The main primary minerals in well OW-35 include: volcanic glass, olivine, sanidines, plagioclase, pyroxene and opaques. Note that the volcanic glass, which is an important constituent of these rocks, is not a mineral in the strict sense, but is very relevant in this
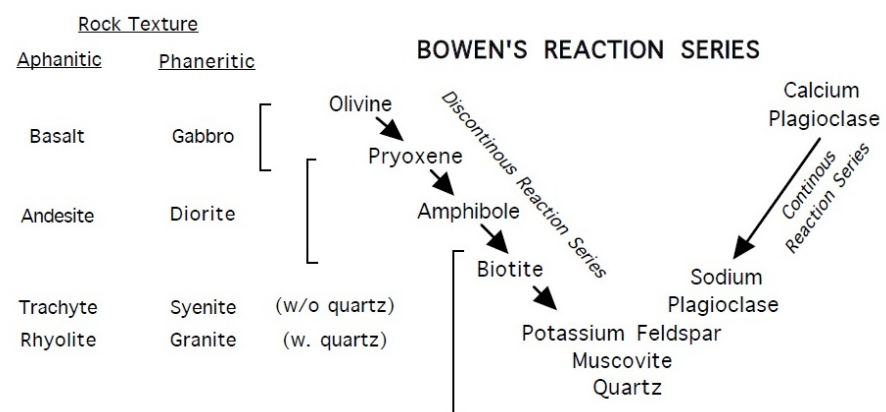


FIGURE 12: Bowen's reaction series (from Thomas, 2010)

discussion as its replacement products are important hydrothermal minerals.

The susceptibility of the primary minerals observed in this well to alteration are conformable with the sequence observed by Browne (1984a and b).  In the order of decreasing susceptibility are: volcanic glass, olivine, pyroxenes, plagioclase/sanidine and opaques.  This is briefly described below:

**Volcanic glass**:  Obsidian, although this type of volcanic glass is not the only naturally occurring volcanic glass.  The conversion of volcanic glass to secondary alteration products is one of the most common mineralogical transformations during low-temperature hydrothermal alteration leading to the formation of clays (Giorgetti et al., 2009).  It is the first primary phase noted in this well to undergo alteration to clays, chalcedony and also replaced by calcite.  This was observed from 124 m in brecciated tuffs and also in basalts.

**Olivine**:  This is a common mineral in basalts but seldom present in trachytes and rhyolites.  Considering the crystallization temperatures of this mineral, it is one of the most susceptible minerals to alteration due to its unstable nature.  Principally, olivine alters to clay such as mixed layer clay; smectite-chlorite, and also significant oxidation can lead to the formation of Fe-oxides (hematite).  This scenario was noted from 382 m in OW-35 depth with calcite as a common replacement mineral.

**Plagioclase**:  It is a primary mineral which occurs mostly as phenocrysts in basaltic groundmass.  It is transparent or when altered milky in colour and has perfect cleavage.  Optically, plagioclase feldspars are distinguished by the distinct polysynthetic twinning pattern of albite and low relief.  Plagioclase is susceptible to alteration and will commonly be sericitized.  Sericite is a fine-grained white mica that is a common alteration product of plagioclase, among others.  Other and more common alteration products of plagioclase in Olkaria basalts include clays, albite, calcite and epidote.

**Sanidine**:  Sanidines are the most dominant feldspars in the trachytic and rhyolitic rocks observed in well OW-35.  Under petrographic analysis, it is colourless, has low relief and is easily distinguished by the distinct simple Carlsbad twinning.  Sanidines are relatively stable at high temperatures but apparently show a characteristic alteration sequence of adularia-albite at the advanced alteration stage.  Notably, this sequence was observed from 1230 m where traces of adularia were spotted replacing sanidine laths.  The alteration was noted to progress from 2654 m with adularia exhibiting partial or complete replacement by albite.  Clays were also noted as alteration products and were very abundant at shallow depths, though they sporadically persisted to the bottom of the well.

**Pyroxenes**:  These are most common in basic rocks and occasionally in acidic rocks.  In well OW-35, they were noted commonly in basaltic formations where they occurred as clinopyroxene phenocrysts in a plagioclase-rich groundmass.  They are usually identified by their inclined extinction pattern under petrography (Saemundsson and Gunnlaugsson, 2002).  They were also common in the syenitic intrusion noted from 2894 m, appearing coarse grained.  In trachytes, aegerine-augite is also common and similarly distinguished by its pleochroism.  Generally, pyroxenes are not susceptible to alteration but with advanced temperatures they alter to amphiboles, mainly actinolite.  In this well, the advanced alteration of pyroxene produced actinolite, which was first noted at 1624 m and extended to the bottom of the well.

**Opaques**:  These are Fe-Ti- oxides.  They crystallized as part of the primary rock constituents.  Opaques are generally resistant to alteration but with progressive temperature increase they alter to clays, sphene, and hematite.  However, magnetite in most places is commonly found near the intrusive bodies as the opaque mineral.

The alteration products of primary minerals are briefly described in Table 4 in the order of their susceptibility to alteration.

TABLE 4: Primary minerals and their alteration products in well OW-35

| Susceptibility | Primary rock minerals | Alteration minerals |
|---|---|---|
| Decreasing | Volcanic glass | Zeolites, chalcedony, clays |
| | Olivine | Amphiboles, chlorite, hematite, clays, pyrite |
| | Feldspar | Adularia, calcite, wairakite, chlorite, epidote, albite, amphiboles |
| | Pyroxene | Actinolite, clays, wollastonite |
| | Opaque | Sphene, hematite, pyrite |

**5.2 Distribution of hydrothermal alteration minerals in well OW-35**

There are broad varieties of hydrothermal mineral assemblages found in this well which are quite similar to what has been observed in other high-temperature fields around the world (Browne, 1978). Below is a detailed description of the hydrothermal alteration minerals encountered in well OW-35.

**Chalcedony**: This is a cryptocrystalline form of silica commonly referred to as an amorphous form of silica. This low-temperature mineral was observed in this well, mostly in vesicles. Chalcedony was noted in different rock types ranging from pyroclastic, rhyolite, trachyte, basalt and tuffs at the upper parts of the well to a depth of about 498 m. Below this depth, chalcedony became unstable, altered and was replaced by quartz, thus indicating formation temperatures greater than 180°C.

**Calcite**: Calcite commonly precipitates in fractures and pores and was found most abundant at shallow depths and as a minor component at greater depths, apparently in vein fillings. The calcite noted from 0-60 m is apparently not related to hydrothermal alteration, since there is no hydrothermal activity taking place at this depth. From 382 to 666 m, it was observed to be abundant as a replacement mineral, principally replacing feldspars and some mafic minerals such as olivines and pyroxenes. Its intensity decreased downwards, occurring as a minor mineral component, and often becoming unstable below 1182 m. In petrographic analysis, calcite is identified by its rhombohedral cleavage and twinkling relief upon rotation of the microscope stage.

**Pyrite**: Pyrite is $Fe_2S$ in composition and occurs as euhedral cubic crystals with a shiny brassy yellow lustre. In this well it was noted to occur at almost all depths, which may indicate good permeability in the well. It was observed to be abundant from 560 to 634 m mainly in basaltic and acidic tuff formations, indicating high permeability in this zone. Below this depth, pyrite occurred as disseminations in the groundmass and in minor proportions. Pyrite is an opaque mineral in thin sections.

**Siderite**: This is a $FeCO_3$ mineral and occurs as reddish-brown aggregates of spherules with a radiating pattern showing a vitreous-silky lustre. In petrography, siderite is discerned to be uniaxial (-ve) with high relief. In this well, it was first noted at 248 m and disappeared at 838 m where it became unstable due to increased temperatures.

**Zeolites**: Zeolites are hydrous secondary minerals composed of Na-K-Ca alumina-silicates. Zeolites form at relatively low temperatures (<120°C). Different varieties of zeolites can be distinguished by their shape, mainly fibrous/acicular, tabular/prismatic and granular (Saemundsson and Gunnlaugsson, 2002). In this well, zeolites were not widely seen, but a fibrous type (mesolite) was noted at 244 m and disappeared with increased temperatures.

**Quartz**: It is colourless with apparently indistinct cleavage and conchoidal fracturing being the conspicuous diagnostic features. Under the petrographic microscope, it is seen as uniaxial (+ve) and is easily identified by its undulating extinction feature. In this well, quartz was first noted at 288 m as a

secondary mineral, often replacing chalcedony. Quartz is usually unaltered even at great depth and is observed precipitating in hydrothermal veins and vesicles.

**Epidote**:  The first appearance of epidote was noted at 678 m in a tuffaceous formation indicating temperatures above 240°C and persisted through to the bottom of the well.  It is usually yellowish green in the binocular analysis with distinct crystal faces.  Under the petrographic microscope, it is distinguished by high interference colours and strong pleochroism.  Epidote is the alteration product of feldspars, micas, pyroxenes and amphiboles among others, and its first appearance indicates the well has entered the geothermal reservoir.  Hence, its appearance is important in deciding the depth of the production casing.

**Chalcopyrite**:  It is brassy to golden yellow in colour and often resembles pyrite, though distinguished from it by the tetragonal crystal structure.  The distinct characteristic feature noted with chalcopyrite in this well is that it occurred in close association with epidote from 728 m, which could also indicate a possible geothermometer and a subject for further research.

**Wairakite**:  This is a high-temperature variety of a zeolite which is usually the calcium rich analogue of analcime.  It is colourless to white with a vitreous dull lustre.  Wairakite is stable at temperatures of 200-250°C.  In this well, it was noted at 1222 m but rarely discerned in thin sections.  The polysynthetic twinning lamella is the conspicuous diagnostic feature.

**Albite**:  It is milky white (cloudy) in appearance, has a euhedral shape and was often observed replacing primary minerals, K-feldspars (sanidine) and plagioclase feldspars, a process referred to as albitisation indicating temperatures above 180°C.  It was observed from 624 m in basaltic formation replacing the plagioclase feldspars and occurred intermittently to the bottom of the well.  Albite was also observed at depths replacing adularia at high temperatures.  In thin sections, it has a cloudy appearance, low refractive indices and its formation involves the destruction of the characteristic plagioclase feldspar twinning habit.

**Adularia**:  Adularia is easily distinguished by sub-hedral to anhedral diamond shaped crystals.  It was observed between 1230 and 2654 m, mainly replacing sanidine feldspar but occasionally deposited in veins.  Below 2654 m, it disappeared and apparently was replaced by albite as the temperatures advanced.

**Sphene**:  Sphenes are colourless with an acute rhombic cross-section.  They were first observed at 1232 m as disseminations in the rock matrix, an indication of temperatures greater than 200°C.  In petrographic microscope, they were recognized as alteration products of opaques and were well dispersed to the bottom of the well.  Sphene appears colourless with an acute rhombic cross-section.  It has high-order interference colours.  It was disseminated in the rock matrix.

**Prehnite**:  It is a high-grade alteration mineral formed at temperatures above 240°C.  It is colourless to grey to yellow-green with a distinct vitreous-pearly lustre.  It was first noted at 994 m, down to 2046 m and was sparsely distributed within this depth range.  In thin sections, it is easily distinguished by strong birefringence and a characteristic bow-tie texture.

**Wollastonite**:  It is white to colourless sometimes grey with a distinct tabular crystal habit which appears fibrous and radiating.  It is usually distinguished by vitreous or dull to pearly colour on cleavage surfaces.  In thin section it is observed as clusters of fine needles exhibiting a radiating pattern.  It was first noted from 2064 m in vesicles, indicating temperatures about 270°C.  Though seldom distributed, it was, however, found to occur in close association with epidote and prehnite.

**Actinolite**:  This is one of the high-temperature geothermometers indicating temperatures of about 280°C.  It was first observed from 1624 m in trachytic formation and persisted to the bottom of the well.  Actinolite is the alteration product of pyroxenes and occasionally opaques.  It is pale green to

white occurring as radiating and fibrous crystal aggregates. Under the petrographic microscope, it is fibrous with moderate relief and shows moderate pleochroism to green with good cleavage.

**Clays**: These are the most common alteration products of most primary minerals and rocks observed in this well. They belong to the phyllosilicate group and alter with interaction with some fluids and other factors among which temperature plays a very important role. Different clay types were observed to occur at almost all depths as replacement minerals and fine clay in filling the vesicles.

The different types of clays identified from binocular analysis were later confirmed by petrographic and XRD analysis. A brief description of the clays is indicated in Table 5 and the XRD analyses are presented in Appendix II.

> **Smectite**: This is a low-temperature clay formed below 200°C (Franzson, 2010). Smectite is observed as fine-grained brown to green aggregates, which are easily recognized by the first order interference colours and characteristic feature of extinctions under the petrographic analysis. Smectite was observed to occur mostly in supergene environments to a depth of about 198 m, replacing the primary minerals and occasionally as fillings in vesicles. Through XRD analysis, very distinctive X-Ray diffractory peaks upon different treatment of each individual sample were noted. The most unique distinguishing feature for smectite clay is the swelling nature of the glycolated sample to 17-19 Å peak and further reconstruction/build-up of the heated sample at 10 Å peak on their first order of diffraction. The characteristic peaks notable in this well ranged from 14.78-16.33, 18.37-19.58 and 10.50-10.98 Å for air-dried/untreated, glycolated and heated samples, respectively.

> **Mixed-layer clays (MLC)**: This is an assemblage of clay minerals of two or more intermediate mineral species. The MLC members noted in this well were smectite-chlorite observed from 378 to 678 m. In thin section, they are recognised by green colour, fine- to coarse-grained texture with close resemblance to chlorite but with a conspicuous strong pleochroism. XRD analysis shows characteristic features of both smectite and chlorite, with the first order diffraction peaks at 15.14-16.47, 18.01-18.56 and 10.82-12.25 Å for the untreated, glycolated and heated samples, respectively. The second diffraction peaks showed unstable chlorite peaks at 7.38-7.61 Å for both untreated and glycolated samples with the heated peak collapsing/disappearing (H=0).

> **Chlorite**: This is a medium- to high-temperature replacement product for most of the primary minerals, occurring at temperatures greater than 200°C. It shows variable textural appearances and was noted from 698 to 2798 m. Chlorites are usually recognized in thin sections by their light green colour, and weak pleochroism with moderate relief. They, however, exhibit variable interference colours from blue-purple-brown. XRD analysis showed two types of chlorite, both the stable and unstable forms with characteristic peaks at 12.43-16.28 Å for all samples: untreated, glycolated and heated samples for the first order diffraction. The second order of diffraction showed peaks at 7.24-7.75 Å for both untreated and glycolated samples with the heated peak collapsing (H=0) in the unstable chlorite.

> **Illite**: Illite clays have extensive distribution in this well, occurring at almost all depths in close association with chlorite. It was first observed from 198-280 m and then from 598 m to the bottom of the well. Notably, illite appears to be stable at high temperatures and often dominates the lower part of the well from 2798 m in vein fillings and also as the common replacement mineral of K-feldspars. In thin sections, it is discerned as colourless to yellow-brown with irregular mottled flakes of crystals and low refractive index.

The distribution of hydrothermal alteration mineralogy in well OW-35 is shown in Figure 13.

FIGURE 13:  Hydrothermal alteration minerals in well OW-35

TABLE 5: Summary of the categorized clay mineral assemblages

| Depth interval (m) | Clay mineral assemblage |
|---|---|
| 0-198 | Smectite |
| 378-678 | MLC (smectite-chlorite) |
| 698-2780 | Chlorite |
| 198-280 and 598-2988 | Illite |

## 5.3 Paragenesis and mineral deposition sequences

Paragenesis is a petrologic concept meaning an equilibrium assemblage of mineral phases. The paragenetic sequence in mineral formation is an important concept in deciphering the detailed geologic history and chronology of hydrothermal ore deposition as well as the evolution of a geothermal system (Guilbert and Park, 1986). The sequence is worked out through detailed microscopic studies in polished ore mineral section, petrologic thin section and fluid inclusion studies as well as macroscopic field relations, particularly involving the cross-cutting relationships in vein fillings. The vein fillings were first noted at 124 m in the form of cryptocrystalline silica with smectite clays and were intermittently distributed to the bottom of the well, often characterized by quartz veins and chlorites as the temperatures advance beyond 200°C. Table 6 summarizes the alteration sequences of mineral deposition.

TABLE 6: Alteration sequences of mineral deposition in well OW-35

| Depth (m) | Lithology | Alteration intensity | Alteration sequence Older ⟶ Younger |
|---|---|---|---|
| 244 | Trachyte | Little | Zeolite- chlorites |
| 288 | Trachyte | Little | Chalcedony-quartz |
| 530 | Basalt | Moderate | Smectite-chlorite |
| 678 | Tuff | Moderate | Sanidine-epidote-chlorite |
| 1222 | Basalt | Moderate | Plagioclase- albite-epidote-chlorite |
| 1624 | Tuff | High | Magnetite-titanite/sphenes-illite |
| 2064 | Trachyte | High | Epidote-wollastonite-Actinolite |
| 2204 | Rhyolite | High | Pyroxene-chlorite-Actinolite |
| 2656 | Trachyte | High | Sanidine-adularia-albite-chlorite |
| 2784 | Trachyte | High | Epidote-prehnite-Actinolite-chlorite |
| 2802 | Rhyolite | High | Chlorite-epidote-actinolite |

## 5.4 Alteration mineral zonation

A summary of the binocular, petrographic and XRD analysis results reveals four mineral alteration zones. The first appearances of the high-temperature geothermometers were used to define the alteration boundaries. A detailed description of these zones is briefly presented below.

*Unaltered zone (0-38 m):* The rocks in this zone are relatively unaltered and the alteration minerals observed in this zone are not related to any hydrothermal activity. It is, however, inferred that the alteration present in this zone is possibly related to mechanical weathering or changes in atmospheric conditions often affecting the supergene environments.

*Smectite – zeolite – illite zone (38-198 m):* Smectite and zeolites are low-temperature minerals usually stable at a temperature less than 200°C. Zeolites were noted at 244 m while smectite clays were identified from XRD analysis to occur from the top to a depth of 498 m.

*Smectite – chlorite (MLC) zone (198-678 m):* This layer is defined by the occurrence of two intermediate clay types, mainly smectite and chlorite at a depth of 498 m. Through XRD analysis, chlorite and illite were observed to occur intermittently to a depth of 648 m, indicating alteration temperatures of about 200°C.

*Epidote – chlorite – illite zone (678-1624 m):* The first appearance of crystalline epidote is very important since it marks the upper boundary of the reservoir. It was first noted in cuttings from binocular analysis at 678 m, indicating reservoir temperatures of more than 240˚C.

*Actinolite – epidote – chlorite – illite zone (1624-3000 m):* The first appearance of actinolite is used to mark the upper boundary of this zone. It was first observed at 1624 m in a thin section and also by binocular analysis, indicating alteration temperatures above 280°C.

## 5.5 Fluid inclusions in well OW-35

Fluid inclusions are microscopic droplets of liquid and/or gas trapped within crystals. They are generally less than 0.1 mm in size and occur in a wide variety of earth environments (Santosh et al., 2008). Fluid inclusion studies have been widely used in borehole geology to provide information on the densities and the composition of fluids trapped in minerals and also to obtain data that can be used to estimate the prevailing temperature and pressure conditions when the fluid was trapped. At ambient temperatures, some inclusions contain a liquid aqueous solution and a gas bubble. This bubble forming process can be reversed to determine the temperature of mineral formation or temperature of homogenization ($T_h$) (Lagat, 2004). The inclusion is heated until the fluid homogenizes into a single phase (i.e. bubble disappears) and the $T_h$ is established.
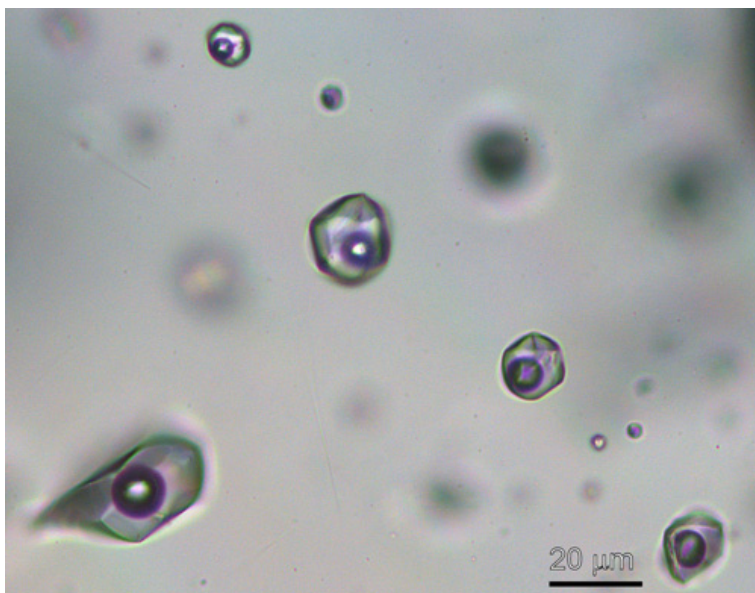


FIGURE 14: Fluid inclusion phases (note the bubbles shown here are similar to those observed in well OW-35) (BGS, 2013)

Fluid inclusions are widely known for occurring in quartz and calcite veins in hydrothermal deposits, as shown in Figure 14. However, they can occasionally be found in minerals that cement sedimentary rocks, in fossil amber and stalactites. The fluid inclusions can be either primary or secondary, the former meaning that they were formed within the first-order growth discontinuities or often occurring as isolated inclusions distributed within the crystal (Roedder, 1984), while the latter means that they formed/were trapped after the primary growth, often along the healed micro-fractures (Lagat, 2004),

Fluid inclusion analysis for this well was carried out on selected individual crystals of quartz picked out from cuttings at depths of 644-646 and 1722-1724 m (see Table 7). A total of 56 measurements were carried out with the highest temperature noted at 310°C. The interpreted fluid inclusion graphs are presented below in Figures 15 and 16, respectively. Figure 17 shows the relationship between measured, boiling point curve, fluid inclusion and alteration mineral temperatures at different depths.

TABLE 7: Fluid inclusion measurements in well OW-35

| Depth 644-646 m | | Depth 1722-1724 m | |
| --- | --- | --- | --- |
| Temp. range (°C) | Inclusions | Temp. range (°C) | Inclusions |
| 210-215 | 2 | 270-275 | 1 |
| 215-220 | 5 | 275-280 | |
| 220-225 | 3 | 280-285 | 9 |
| 225-230 | 7 | 285-290 | 3 |
| 230-235 | 4 | 290-295 | 6 |
| | | 295-300 | 8 |
| | | 300-305 | 5 |
| | | 305-310 | 3 |
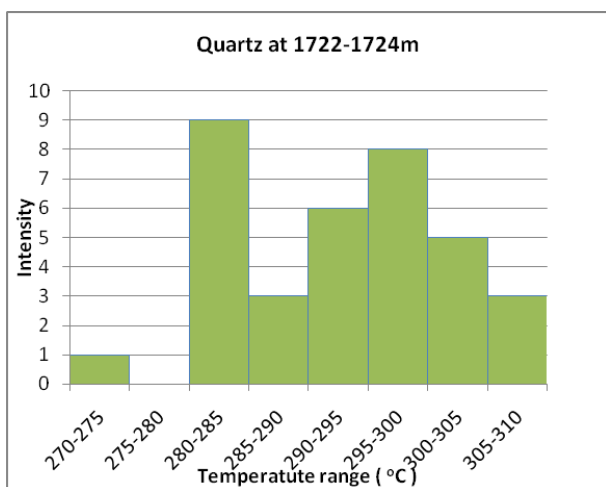


FIGURE 15: Fluid inclusion measurements in quartz collected at 1722-1724 m
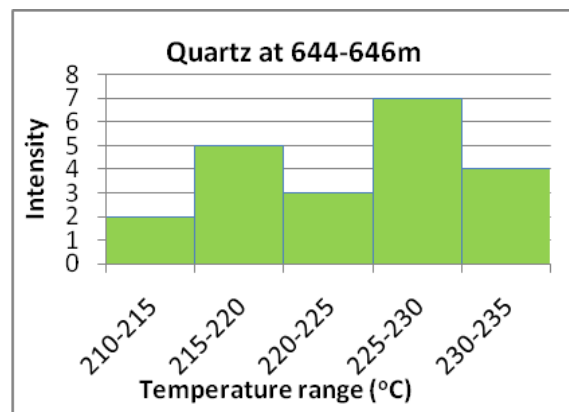
FIGURE 16: Fluid inclusion measurements in quartz collected at 644-646 m

From the correlation above, it is evident that, the well is at an equilibrium state at a depth of 1000 m, where the measured, alteration and the boiling temperatures are the same. It is also noted that, above 1000 m the homogenization, alteration and the measured temperature of the well are above the boiling conditions. Between 1000 and 2000 m, the well is observed to be heating up as the alteration temperatures are lower than the measured and homogenization temperatures. Generally, the homogenization temperatures for both inclusions at 646 and 1724 m reflect more or less the present conditions of the system with the measured temperatures of 234 and 288°C being close to the average fluid inclusion homogenization temperatures of 227.5 and 297.5°C, respectively.

From a comparison of alteration and measured temperatures, it is clear that there are observable feed zones in the depth range of 1550-1800 m, where the alteration temperature is slightly below the measured temperature, an indication that the system is slightly heating at the upper column of the well. Similarly, within this zone there is a distinct rise in temperature, a fact that could be interpreted as the location of the best feed zone. Below this depth, sudden inferred cooling (not sufficient heat-up time allowed) was observed, evidenced by the alteration temperature being greater than the measured temperature, followed by a convective cell down to 2400 m where subsequent knee hikes (inferred several aquifers) were noted and progressed to the bottom of the well.
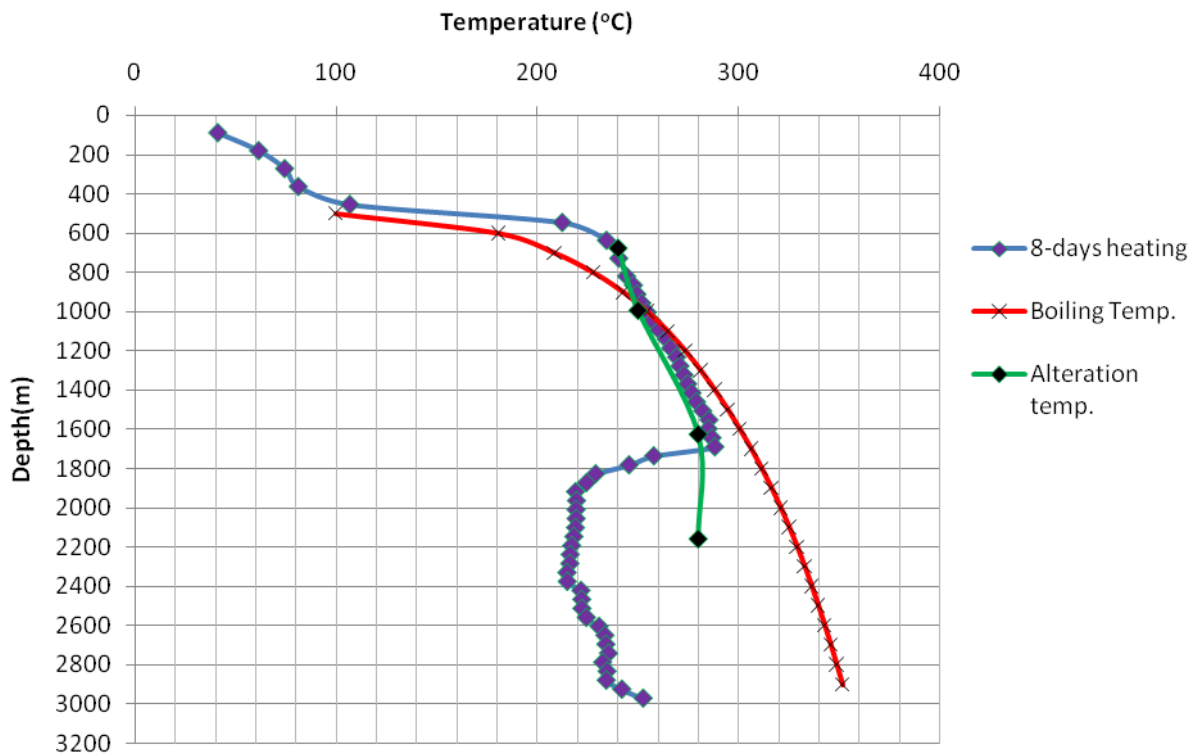
FIGURE 17:  The relationship between fluid inclusion temperature, alteration minerals temperature
and boiling point curve for well OW-35;  the measured temperature readings were taken 8 days after
injection tests, hence the curve may be inaccurate, probably showing too low temperatures,
as the well may not have reached equilibrium with the surrounding rock formations

## 5.6  Pressure and temperature logs

Pressure and temperature logs are used to determine reservoir characteristics in a well.  Strictly
speaking, the best feed zone in a well has equilibrium pressure since it portrays the true reservoir
pressure.  It is in these regions where the reservoir is in communication with the well (Björnsson,
2012).

The KenGen reservoir scientists carried out step pumping on 20th November, 2010, using an adjustable
high-pressure pump.  They pumped water into the well while varying the pumping rate in controlled
step tests.  The first pumping rate was 1000 lpm, increased to 1300 lpm, then 1600 lpm and finally
1900 lpm.  Pumping was done for four hours for the first step and three hours in the consequent steps.
The down-hole pressures were plotted against corresponding pumping rates to determine
transmissivity and storativity, which would give an indication of the permeability of the well.

According to Stefánsson and Steingrímsson (1990), feed zones warm up much more slowly than the
host compact country rock, making them easily identifiable from temperature logs.  In well OW-35,
good feed zones were noted in the upper production section of the well between 950 and 1800 m,
where there was continuous change in fluid interaction temperature conditions during a pre-injectivity
test and injectivity testing.  The pressure in this region was, however, very stable and uniform during
these tests, hence this indicates that the upper region has the best feed zone.  After the injectivity tests,
there was an observable heat up due to inflow, a concise indication that the well is in proper
communication with the reservoir.

Generally, below 2400 m, there are several small feed zones, apparently characterrized by sharp kinks with the dominant one noted at 2900 m, which probably portrays a relatively bigger feed zone. However, the temperature logs after 8 days could indicate that the flow in the well has been reversed. Further, the pressure logs indicate that the best feed zones are between 1550 and 1800 m. However the logs were done very soon after drilling was completed. The top feed zone could possibly be yielding steam.

From the pressure profiles, the *water rest level* of well OW-35 is estimated to be at 500 m. Lagat (2004) concluded that this is where boiling conditions of the well were inferred to begin. As, in most areas, the sub-surface fractures, fissures, faults and strata contacts form the main feed zones, a fact supported by temperature and pressure logs carried out in well OW-35 (see Figure 18).
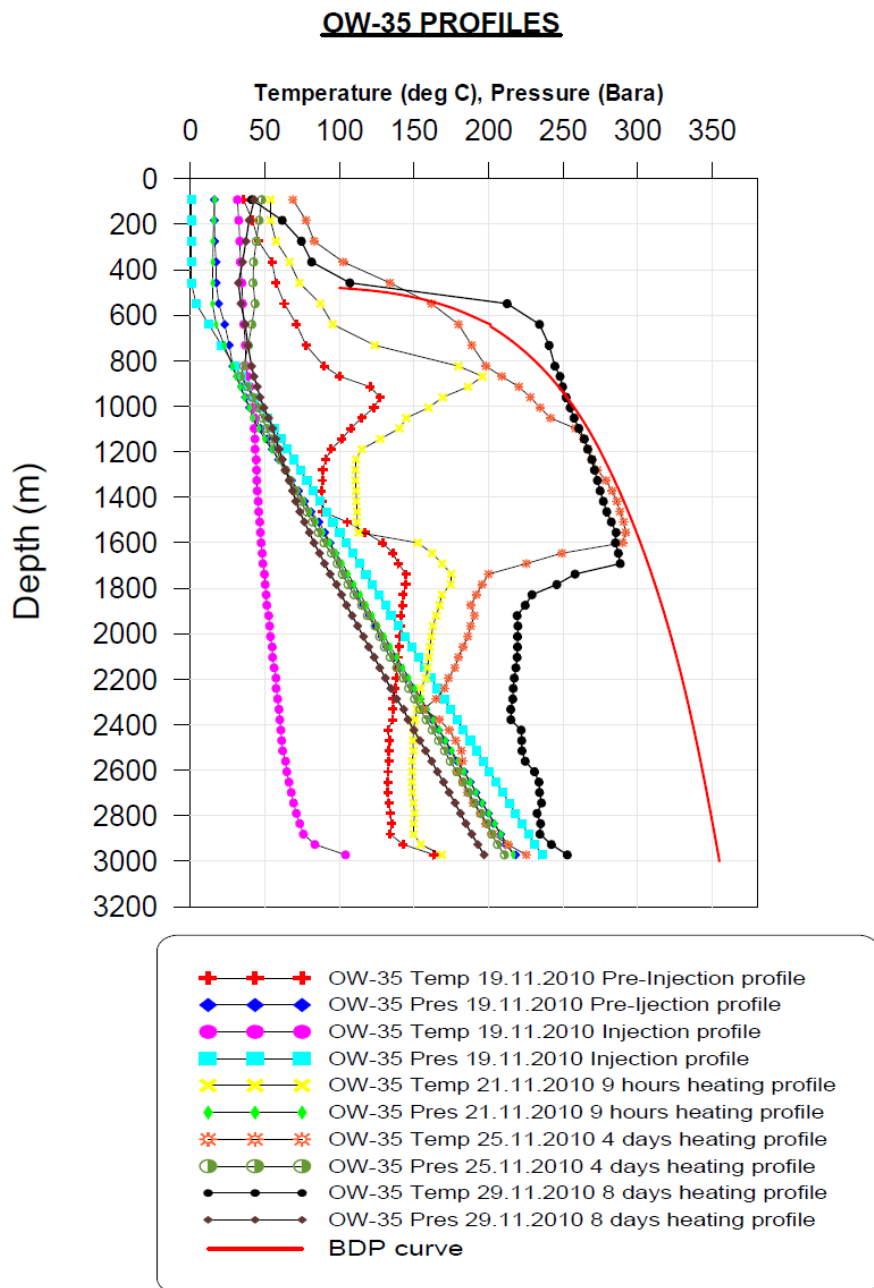


FIGURE 18: Pressure and temperature profiles of well OW-35

## 6. LITHOSTRATIGRAPHIC CORRELATION AND ALTERATION ZONATION BETWEEN WELLS OW-35 AND OW-37A

Wells OW-35 and OW-37A were drilled in Olkaria East production field at altitudes of 2017 and 1960 m a.s.l., respectively, and encountered rock types at similar depths with slight differences apparently due to tectonic activity. The basaltic lava flow which defines the caprock of the reservoir has been used as the marker horizon as it is widespread.

Between wells OW-37A and OW-35, basaltic lavas were encountered at 1549 and 1432 m a.s.l., respectively. This accounts for total displacement at 117 m to the east, inferred as a fault zone (Figure 19). According to Lagat's conceptual model of the Olkaria geothermal field (2004), a normal fault was found between these two wells; this coincides with our observation.
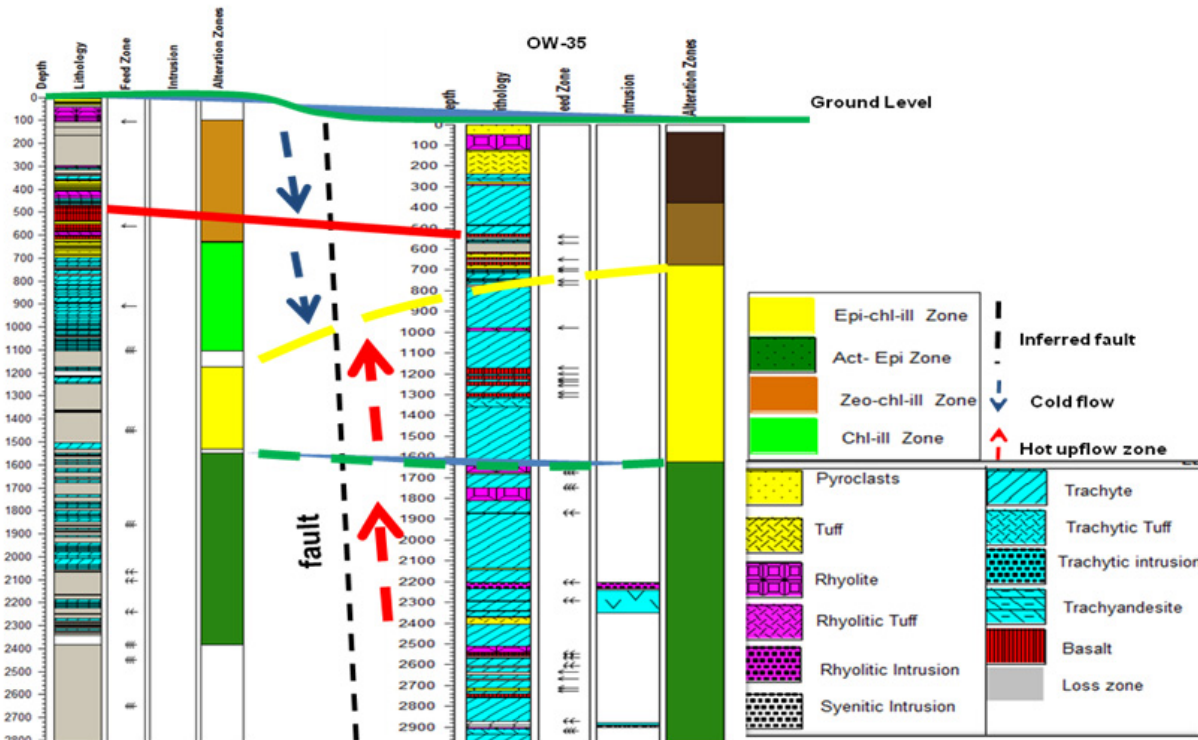


FIGURE 19: Stratigraphic correlation models for wells OW-37A and OW-35

Epidote and actinolite are the two geothermometers used for correlation between wells OW-37A and OW-35 with the first appearance of epidote at 1172 in OW-37A and 678 m in OW-35, while actinolite appeared at 1548 m (OW-37A) and 1624 m (OW-35), respectively (see Figure 19). It can be seen from Figure 19 that the alteration is found at shallower levels in well OW-35. This difference is inferred by a possible cold down-flow near well OW-37A and/or a hot upflow-zone in the vicinity of well OW-35, though further correlation to neighbouring wells are required to confirm this.

## 7. DISCUSSION

The stratigraphy of well OW-35 consists of pyroclastics, tuffs and breccia, rhyolites, trachytes, trachy-andesites, basalts and rhyolite and syenite intrusions. Trachytes are the dominant lava rocks in this field, more voluminous than the other lavas observed. There are two types of rhyolites encountered in this well: extrusive and intrusive rhyolites. The former are fine grained, weakly porphyritic and susceptible to alteration, while the intrusives are medium to coarse grained, with euhedral sanidine and quartz crystals and appear relatively fresh. Riebeckite was more abundant in rhyolitic intrusions than in the lava flows. The variance is attributed to the rate of cooling of the rocks. Two varieties of trachyte were recognised based on the degree of alteration, apparently related to the thermal gradient.

Several geothermometers were used to predict the prevailing temperature conditions of the well. These include: epidote, quartz, wairakite, wollastonite, prehnite and actinolite. Their expected alteration temperatures were compared with measured temperatures and further correlated with fluid inclusion-homogenization temperatures. The first appearances of these minerals were noted as

follows. Epidote was first noted in the well at 678 m, which is very close to the end of the production casing. This means that the formation temperatures at that depth were expected to be above 240°C. Other high-temperature minerals include: prehnite (>230°C), wairakite (>200°C), actinolite (280°C), and wollastonite (~270°C). These minerals were first encountered at 994, 1222, 1624 and 2064 m, respectively. From a comparison of these alteration temperatures with measured and homogenization temperatures, it is evident that the system is in equilibrium, often inferred from the close proximity among the trends.

According to Lagat (2004), hydrothermal minerals are likely to be found in close association with veinlets, vugs and as replacements of primary minerals in the volcanic rocks. Their occurrence and extent is similar to the prograde variations observed in other geothermal fields in the world. Clays are widely used as indicators of previous subsurface conditions in geothermal systems. This has made them receive acknowledgement as good geothermometers. Clays in well OW-35 were observed as infills and replacement minerals. They occurred from 48 m to the bottom of the well, with illite being the most dominant. They have proven to be useful in particular temperature estimations. The regular change with depth seen in this well is from smectite – MLC (smectite-chlorite) – chlorite – illite. Both stable and unstable chlorites were also prevalent, often in random distribution in all types of formations encountered in this well.

From hydrothermal alteration mineralogy, it is evident that the patterns have a notable variation with depth with four distinct hydrothermal mineral zonations; in the order of increasing depth, the zones occur as follows: smectite-zeolite-illite (1st), smectite-chlorite (MLC 2nd), epidote-chlorite-illite (3rd) and actinolite-epidote-chlorite-illite zone (4th). They were encountered at the following depths: 38-198, 378-678, 678-1624 and 1624-2988 m, respectively.

Geochemical data analyses show chloride-rich waters in well OW-35. This would imply mature waters that have interacted with the reservoir. Chloride-rich waters are indicators of upflow zones in a reservoir. From the geochemical fluid data obtained, the well has Cl⁻ concentrations ranging from 300 to 600 ppm.

The temperature-pressure logs also provide information on the subsurface conditions. The 8 day heating curve displayed maximum temperatures of 288°C. The pressure profiles showed good interaction with the reservoir at depths between 1550 and 1800 m. This equilibrium state signifies constant communication with the reservoir, resulting in good production of about 6-8 MW.

A marker horizon in the stratigraphy of wells OW-37A and OW-35 indicates that there is a displacement between the two wells. A normal fault with a total displacement of 117 m to the east was observed. Alteration minerals show that alteration zones were found at a shallower depth in well OW-35, a difference inferred by a possible cold down-flow near well OW-37A and a hot upflow-zone in the vicinity of well OW-35.

Generally, from the data collected and analysed, it is likely that well OW-35 has high prospects in terms of mass flow. The regional geology supports the siting of this well in close proximity to a heat source and in permeable strata. These two conditions are very important in geothermal production. The alteration mineralogy has shown the presence of zonations throughout the well profile, a condition showing proximity to a heat source at depth.


## 8. CONCLUSIONS

The objectives of this study were met by examining the lithology, hydrothermal mineralisation, sequences of mineral deposition in veins and vesicles, locations of aquifers, and the temperature

conditions of the reservoir in well OW-35. This report is also a requirement stipulated by the United Nations University Geothermal Training Programme in advanced training in borehole geology.

The lithostratigraphy of the Olkaria East field is composed of pyroclastics, tuffs, rhyolites, trachytes and basalts with minor rhyolitic, trachytic and syenite intrusives. This lithology is consistent with other fields in GOGA.

The Olkaria East field is intersected by two major faults, namely Olkaria and Olbutot faults, though there are other localized structural lineaments traversing the field in general NE-SW and E-W directions. Sources of permeability in this field are both primary and secondary and include: fractures and thermally induced joints, lithologic contacts, clast-matrix or fragment contacts in breccias and scoraceous fragments.

The high alteration intensity, fissured rocks, vein fillings, and pyrite and calcite abundance define the permeability pattern in this well.

Chemical data analysis for well OW-35 shows high $Cl^-$ concentrations, a phenomenon related to the close proximity of a heat source. These findings are also supported by the conceptual model shown in Figure 8.

From the occurrence and zonation of hydrothermal alteration and mineralogical assemblages in this well, it is evident that they are mainly controlled by temperature, rock type and permeability. There were four distinct zones noted. Zonations show a progression pattern of hydrothermal reactions with depth.

Comparison between measured, alteration and homogenization temperatures depicts a state of equilibrium in the well.

There are several feed zones in this well characterised by temperature kinks in the measured profiles. The best feed zones encountered in this well were between 1550 and 1800 m and from 2900 to 3000 m. These feed zones were interpreted to be the significant communication channels between the well bore and the reservoir.

The marker horizons in the stratigraphy of wells OW-37A and OW-35 indicate that there is a displacement between these two wells. A normal fault with a total displacement of 117 m to the east was observed. Alteration minerals show that alteration zones were found at a shallower depth in well OW-35, a difference inferred by a possible cold down-flow near well OW-37A and/or a hot upflow-zone in the vicinity of well OW-35.


## ACKNOWLEDGEMENTS

# REFERENCES

Baker, B.H., Mohr, P.A., and Williams, L.A.J., 1972: Geology of the Eastern Rift System of Africa. *Geological Society of America, Special Paper 136,* 1-67.

Baker, B.H., Williams, L.A.J., Miller, J.A., and Fitch, F.J., 1971: Sequence and geochronology of the Kenya Rift volcanics. *Tectonophysics,* 11, 191-215.

Baker, B.H., and Wohlenberg, J., 1971: Structural evolution of the Kenya Rift Valley. *Nature, 229,* 538-542.

Björnsson, G., 2012: *Using temperature and pressure logs to determine reservoir condition and well status.* UNU-GTP, Iceland, unpublished lecture notes.

Braun, H.M.H., 1980: *Agro-climatic zone map of Kenya.* Ministry of Agriculture, Appendix 2 to report No. E1.

BGS, 2013: *Fluid inclusion phases.* British Geological Service, website: *www.bgs.ac.uk,* (accessed on 8.1.2013).

Browne, P.R.L., 1978: Hydrothermal alteration in active geothermal fields. *Annual Reviews of Earth and Planetary Science, 6,* 229-250.

Browne, P.R.L., 1984a: Subsurface stratigraphy and hydrothermal alteration of Eastern section of the Olkaria geothermal field, Kenya. *Proceedings of the 6th New Zealand Geothermal Workshop, Auckland, NZ,* 33-41.

Browne, P.R.L., 1984b: *Lectures in geothermal geology and petrology.* UNU-GTP, Iceland, report 2, 92 pp.

Chorowicz, J., 2005: The East African rift system. *J. African Earth Science, 43, 1-3,* 379-410.

Clarke, M.C.G., Woodhall, D.G., Allen, D., and Darling, G., 1990: *Geological, volcanological and hydrogeological controls of the occurrence of geothermal activity in the area surrounding Lake Naivasha, Kenya.* Ministry of Energy report, Kenya.

Driscoll, F.G., 1986: *Groundwater and wells* (2nd ed). Johnson Division, 1089 pp.

Franzson, H., 2010: *Borehole geology.* UNU-GTP, Iceland, unpublished lecture notes.

Giorgetti, G., Monecke, T., Kleeberg, R., and Hannington, M.D., 2009: Low-temperature hydrothermal alteration of trachybasalt at conical seamount. Papua New Guinea: Formation of smectite and metastable precursor phases. *Clays and Clay Minerals, 57,* 725-741.

Guilbert, J.M., and Park, C.F., 1986: *The Geology of ore deposits.* W.H. Freeman, NY, 999 pp.

Gylfadóttir, S.S., Halldórsdóttir, S., Arnaldsson, A., Ármannsson, H., Árnason, K., Axelsson, G., Einarsson, G.M., Franzson, H., Fridriksson, Th., Gudlaugsson, S.Th., Gudmundsson, G., Hersir, G.P., Mortensen, A.K., and Thordarson, S., 2011: *Revision of the conceptual model of the Greater Olkaria geothermal system– Phase I.* Mannvit/ÍSOR/Vatnaskil/Verkís, Reykjavík, June, 100 pp.

Hardarson, B.S., 2012: The East African Rift Valley. UNU-GTP, Iceland, unpublished lectures.

Karingithi, C.W., 1996: *Olkaria East production field geochemical report*. Kenya Power Company, internal report.

Lagat, J.K., 2004: Geology, hydrothermal alteration and fluid inclusion studies of the Olkaria Domes geothermal field, Kenya. University of Iceland, MSc thesis, UNU-GTP, Iceland, report 2, 71 pp.

Lichoro, C.M., 2009: Joint 1-D inversion of TEM and MT data from Olkaria Domes geothermal area, Kenya. Report 16 in: *Geothermal training in Iceland 2009*. UNU-GTP, Iceland, 289-318.

Macdonald, R., Belkin, H.E., Fitton, J.G., Rogers, N.W., Nejbert, K., Tindle, A.G., and Marshall, A.S. 2008: The roles of fractional crystallization, magma mixing, crystal mush remobilization and volatile-melt interactions in the genesis of a young basalt-peralkaline rhyolite suite, the Greater Olkaria Volcanic Complex, Kenya rift valley. *J. Petrology, 49,* 1515-1547.

Marshall, A.S., MacDonald, R., Rogers, N.W., Fitton, J.G., Tindle, A.G., Nejbert, K., and Hinton, R.W. 2009: Fractionation of peralkaline silicic magmas: the Greater Olkaria Volcanic Complex, Kenya Rift Valley. *J. Petrology*, *50*, 323-359.

Mechie, J., Keller, G.R., Prodehl, C., Khan, M.A., and Gaciri, S.J., 1997: A model for the structure, composition and evolution of the Kenya rift. *Tectonophysics, 278*, 95-118.

Mungania, J., 1992: *Preliminary field report on geology of Olkaria volcanic complex with emphasis on Domes area field investigations*. Kenya Power Company internal report.

Naylor, W.I., 1972: *Geology of the Eburru and Olkaria prospects*. UN Geothermal Exploration Project, report.

Odongo, M.E.O., 1993: A geological review of Olkaria geothermal reservoir based on structure. *Proceedings of the 15th Geothermal Workshop, Auckland, New Zealand*, 169-173.

Omenda, P.A., 1994: The geological structure of the Olkaria west geothermal field, Kenya. *Stanford Geothermal Reservoir Engineering Workshop, 19, Stanford,* 125-130.

Omenda, P.A., 1998: The geology and structural controls of the Olkaria geothermal system, Kenya. *Geothermics, 27-1,* 55-74.

Omenda, P.A., 2000: Anatectic origin for comendite in Olkaria geothermal field, Kenya Rift; Geochemical evidence for syenitic protholith. *African J. Science & Technology. Science and Engineering Series, 1,* 39-47.

Roedder, E., 1984: Fluid inclusions. *Reviews in Mineralogy, 12*, 3-10.

Rogers, N., Macdonald, R.J., Fitton, G., George, R., Smith, M., and Barreiro, B., 2000: Two mantle plumes beneath the East African rift system Sr, Nd and Pb isotope evidence from Kenya Rift basalts. *Earth Planet. Sci. Letts., 176*, 387-400.

Saemundsson, K., and Gunnlaugsson, E., 2002: Icelandic rocks and minerals. Edda and Media Publishing, Reykjavík, Iceland, 233 pp.

Saggerson., 1963: *Geology of the Naivasha area*. Report no. 64, Government Press, 33 pp.

Santosh, M., and Omori, S., 2008: $CO_2$ windows from mantle to atmosphere: Models on ultrahigh-temperature metamorphism and speculations on the link with melting of snowball Earth. *Gondwana Research, 14,* 82-96.

Simiyu, S.M., 1999:  Seismic velocity analysis in the Olkaria geothermal field.  *Proceedings of the 24ᵗʰ Workshop on Geothermal Reservoir Engineering, Stanford University, Stanford,* 7 pp.

Simiyu, S.M., and Keller, G.R., 1997:  Integrated geophysical analysis of the East African Plateau from gravity anomalies and recent seismic studies. *Tectonophysics, 278,* 291-314.

Simiyu, S.M., Omenda, P.A., Keller, G.R., and Anthony, E.Y., 1995:  Geophysical and geological evidence for the occurrence of shallow magmatic intrusions in the Naivasha sub-basin of the Kenya rift.  *AGU Fall 1995 Meeting Abst., F657, no.  V21A-12.*

Smith, M., 1994:  Stratigraphic and structural constraints on mechanisms of active rifting in the Gregory Rift, Kenya.  In:  Prodehl, C., Keller, G.R., and Khan, M.A., (eds.), Crustal and upper mantle structure of the Kenya rift.  *Tectonophysics, 236*, 3-22.

Smith, M., and Mosley, P., 1993:  Crustal heterogeneity and basement influence on the development of the Kenya rift, East Africa.  *Tectonics, 12*, 591-606.

Stefánsson, V., and Steingrímsson, B.S., 1990: *Geothermal logging I, an introduction to techniques and interpretation* (3ʳᵈ ed.).  Orkustofnun, Reykjavík, report OS-80017/JHD-09, 117 pp.

Thomas, J., 2010: *Fairly simple geology exercises for students and their teachers.*  Skidmore College, website, *www.skidmore.edu.*

Virkir-Sweco., 1980:  *Feasibility report for the Olkaria geothermal project.*  UN - Government of Kenya report.

Wheeler, W.H., and Karson, J.A., 1994:  Extension and subsidence adjacent to a "weak" continental transform:  an example of the Rukwa Rift, East Africa.  *Geology, 22,* 625–628.

Williams, L.A., and Crerar, D.A. 1985: Silica diagenesis, II. General mechanisms. Journal of Sedimentary Petrology. 55, 3, 312 - 321.

**APPENDIX I:  Lithologic description and hydrothermal alteration minerals in well OW-35**
The list hydrothermal alteration minerals is based on binocular and petrographic microscopes

| Top (m) | Base (m) | Rock description | Rock type | Secondary minerals |
|---|---|---|---|---|
| 0 | 4 | Greyish to brownish unconsolidated rock fragments consisting of soil, glass, pumice, obsidian and lithic material of weathered lava. some of fragments contain clays | Pyroclasts | Calcite |
| 4 | 6 | Same though felsic minerals are abundant. | Pyroclasts | Calcite |
| 6 | 8 | Same but has obsidian and chalcedony. Generally the rock is porous. | Pyroclasts | |
| 8 | 10 | Same but most of the fragments are of rhyolitic origin | Pyroclasts | Calcite |
| 10 | 14 | Same but no calcite and sulphur deposits are noted in the matrix | Pyroclasts | |
| 14 | 22 | Light grey to greenish fine-grained rock fragments, occasionally oxidized with some clays. Fragments are of rhyolitic origin. | Pyroclasts | Chalcedony |
| 22 | 30 | Same with little calcite. | Pyroclasts | Calcite |
| 30 | 36 | Light greenish to greyish fine-grained pyroclastic material. | Pyroclasts | Pyrite |

| Top (m) | Base (m) | Rock description | Rock type | Secondary minerals |
|---|---|---|---|---|
| | | shows abundance of clays and limonite and sulphur deposits. | | |
| 36 | 48 | Light grey to brownish fine-grained, oxidized and porous rock. Shows little sulphur deposits and occasional limonite. | Pyroclasts | Pyrite, oxides, smectites |
| 48 | 56 | Light grey fine-grained slightly oxidized porous rock with phenocrysts of iron oxide and occasional quartz and clays. | Rhyolite | Smectites |
| 56 | 58 | Same but more felsic with some pyrite dissemination. | Rhyolite | Smectites |
| 58 | 60 | Same with calcite, chalcedony and tiny crystals of iron oxides. | Rhyolite | Calcite, chalcedony, smectites |
| 60 | 66 | Same with no calcite. | Rhyolite | Calcite, chalced, smectites |
| 66 | 70 | Same with well-developed crystals of iron oxides, occasional free quartz and feldspar.. Shows fluoride contamination (bluish). | Rhyolite | Calcite, chalced, smectites |
| 70 | 82 | Same with no calcite. | Rhyolite | Pyrite, calcite, smectites |
| 82 | 92 | Same with little calcite and pyrite | Rhyolite | Pyrite, calcite, smectites |
| 92 | 102 | Same with no calcite | Rhyolite | Pyrite |
| 102 | 120 | Whitish to pinkish fine-grained rock, moderately altered and oxidized with some mafic minerals | Rhyolite | Pyrite, calcite, chalced., limoni. smectites |
| 120 | 122 | Same | Rhyolite | Pyrite, smectites |
| 122 | 124 | Light grey to brownish rock with sub-angular fragments cemented in a fine-grained matrix (fault breccia ??). | Breccia | Chalcedony, limonite, smectites |
| 124 | 126 | Yellowish green with fragmented crystalline material. Shows moderate intensity of oxidation (tuffac. breccia ?). | Breccia | Chalcedony, smectites |
| 126 | 130 | Same | Breccia | Smectites |
| 130 | 132 | Most grains are brownish with a few appearing brown. The rock is fine grained and shows slight intensity of oxidation and alteration to clays. | Acid tuff | Chalcedony, smectites, pyrite |
| 132 | 142 | Same but no oxides. | Acid tuff | Pyrite, smectites |
| 142 | 144 | Same, but the yellowish grains are abundant and some occasional quartz grains are noted. | Acid tuff | Pyrite, smectites |
| 144 | 152 | Same, but the yellowish gains are abundant and some occasional quartz grains are noted. | Acid tuff | Chalcedony, pyrite, smectites |
| 152 | 160 | Same though the grains are slightly oxidised and amorphous silica, clays and occasional quartz are noted. | Acid tuff | Chalcedony, smectites |
| 160 | 184 | Same, yellowish green fine grained porous rock with mafic minerals appearing as phenocrysts. | Acid tuff | Chalcedony, smectites |
| 184 | 186 | Yellowish fine-grained moderate to highly oxidised tuff. It is highly altered with occasional well-formed quartz crystals and amorphous silica. | Acid tuff | Chalcedony, smectite |
| 186 | 190 | Same but increased amount of brown with decrease in chlorides | Acid tuff | Chalcedony, smectite |
| 190 | 192 | Same but not oxidised | Acid tuff | Chalcedony, smectite |

| Top (m) | Base (m) | Rock description | Rock type | Secondary minerals |
|---|---|---|---|---|
| 192 | 196 | Same but moderate to highly altered. | Acid tuff | Chalcedony, smectite |
| 196 | 198 | Same but moderately oxidised. | Acid tuff | Chalcedony, smectite |
| 198 | 200 | Same but slightly oxidised. | Acid tuff | Chalced., illite |
| 200 | 202 | Yellowish to reddish fine-grained highly oxidised and altered rock with occasional fresh quartz. | Acid tuff | Chalcedony, illite |
| 202 | 208 | Same but slightly oxidised. | Acid tuff | Chalced., illite |
| 208 | 214 | Yellowish brown fine-grained tuffaceous material, moderately altered with some occasional quartz crystals. | Acid tuff | Chalcedony, illite |
| 214 | 234 | Same but moderate to highly oxidised. | Acid tuff | Chalced., illite |
| 234 | 238 | Yellowish to greyish fine-grained mixed cuttings of tuff, glass and lithic fragments. | Acid tuff | Illite |
| 238 | 246 | Yellowish, light to brown fine-grained mixed cuttings comprising of volcanic glass, tuff and clastic material | Trachyte | Pyrite, illite, zeolites |
| 246 | 260 | Greyish fine-grained feldspar rich with occasional fresh glass. | Trachyte | Chalcedony, siderite, pyrite, illite |
| 260 | 262 | Greyish fine-grained with plagioclase laths and occasional quartz crystals | Trachy-andesite | Pyrite, illite |
| 262 | 264 | Greyish to brownish fine-grained vesicular with phenocrysts of mafic and occasional primary quartz | Trachy-andesite | Pyrite, illite |
| 264 | 268 | Fine-grained rock with plagioclase laths. A thin layer of basaltic origin (intermediate layer) is noted along with occasional quartz. | Trachy-andesite | Pyrite, illite |
| 268 | 274 | Fine-grained rock with plagioclase laths. A thin layer of basaltic origin (intermediate layer) is noted along with occasional quartz. | Trachy-andesite | Pyrite, illite |
| 274 | 286 | Brownish green rock with vesicular fragments composed of fine-grained pyroclastic materials. No infill in the vesicles | Acid tuff | Calcite, hematite, illite |
| 286 | 292 | Light grey crystalline quartz rich tuffaceous rock. It is porous and shows vesicles | Rhyolitic tuff | Calcite, pyrite, quartz, smectite |
| 292 | 302 | Dark grey fine-grained with abundance of K-feldspars (sanidine). It is fractured and shows distinct flow banding | Trachyte | Calcite, pyrite, smectite |
| 302 | 304 | Same, but the rock has some pyroxenes and slightly altered | Trachyte | Calcite, quartz, pyrite, smectite |
| 304 | 322 | Same, but shows slight to moderate intensity of alteration | Trachyte | Pyrite, smectite |
| 322 | 342 | Light grey, fine grained slightly oxidized with tiny pyrite disseminations | Trachyte | Pyrite, smectite |
| 342 | 344 | Dark grey fine-grained rock with slight intensity of oxidation | Trachyte | Pyrite, smectite |
| 344 | 348 | Brownish grey fine-grained rock. It is highly fractured with vein infilled with secondary quarts and feldspars. Tiny pyrite disseminations are noted in the matrix | Trachyte | Smectite, pyrite |
| 348 | 350 | Greyish fine grained with increased intensity of alteration and tiny pyrite disseminations | Trachyte | Quartz, smectite, pyrite |
| 350 | 354 | Brownish grey fine-grained highly fractured rock with veins infilled with secondary quartz | Trachyte | Quartz, smectite, pyrite |

| Top (m) | Base (m) | Rock description | Rock type | Secondary minerals |
|---|---|---|---|---|
| 354 | 360 | Greyish to green, fine-grained moderately altered rock with abundance of clays (probably an interlayer between two lava flows) | Trachyte | Smectite, chalcedony, pyrite |
| 360 | 370 | Dark greyish fine-grained slightly oxidised and altered rock. The rock is vesicular with pyrite particles in the matrix. | Trachyte | Pyrite, smectite |
| 370 | 380 | Greyish to brownish fine-grained moderately altered rock with vesicles infilled with secondary mineral. | Trachyte | Chalcedony, smect., chlorite |
| 380 | 388 | Dark grey to light brown fine-grained small feldspar laths and occasional feldspar phenocrysts. the rock is vesicular. | Basalt | Calcite, pyrite, siderite, smect., chlorite |
| 388 | 428 | Same but with moderate calcite. | Basalt | Calcite, pyrite, siderite, smect., chlorite |
| 428 | 436 | Brownish to greenish fine-grained mixed cuttings of basaltic layer and tuffaceous material. It is moderately oxidised and altered. | Tuff | Calcite, smectite, chlorite |
| 436 | 444 | Dark grey fine grained slightly altered with little oxidation. | Trachyte | Pyrite, calcite, smect., chlorite |
| 444 | 454 | Greyish fine-grained slightly oxidised and altered rock. | Trachyte | Calcite, smect., chlorite, quartz, chalced., oxides |
| 454 | 466 | Same | Trachyte | Quartz, calcite, smect., chlorite, pyrite, oxides |
| 466 | 484 | Mixed cuttings of trachytic composition and tuffaceous material. It is moderately oxidised and slightly altered. | Trachyte | Calcite, pyrite, smect., chlorite |
| 484 | 488 | Light grey fine-grained lithic tuff | Trachytic tuff | Smectite, chlorite, pyrite |
| 488 | 528 | Dark grey fine to medium-grained feldspar rich rock. It is weakly oxidised and altered and shows sequence of zoning | Trachyte | Calcite, pyrite, oxides, smectite, chlorite |
| 528 | 542 | Dark to light grey fine-grained rock with quartz and feldspar phenocrysts. The rock is vesicular and infilled with clays and calcite. | Basalt | Calcite, pyrite, smect., chlorite |
| 542 | 552 | Loss of circulation returns | | |
| 552 | 558 | Light grey fine-grained partly crystalline rock fragments and tuffaceous material with slight intensity of oxidation and alteration | Trachytic tuff | Pyrite, smectite, chlorite, calcite |
| 558 | 564 | Light to dark grey fine-grained mixed cuttings of basaltic and trachytic composition. It shows slight to moderate intensity of alteration.. | Basalt | Pyrite, smectite, chlorite, calcite, oxides |
| 564 | 570 | Greyish to dark green fine-grained rock with occasional feldspar phenocrysts and shows moderate intensity of alteration. | Trachyte | Chlorite, pyrite, calcite |
| 570 | 616 | Loss of circulation returns. | | |
| 616 | 620 | Mixed cuttings of dark grey basaltic lava and light grey feldspar rich trachyte.. | Basalt | Calcite, pyrite, oxides, chlorite |
| 620 | 626 | Mixed cuttings with abundant light grey tuff fragments and | Acid tuff | Calcite, pyrite, |

| Top (m) | Base (m) | Rock description | Rock type | Secondary minerals |
|---|---|---|---|---|
| | | dark grey basaltic cuttings. It is weakly altered. | | smectite, chlorite |
| 626 | 630 | Light grey to dull green lithic material, non-crystalline and moderately altered to green clays. | Acid tuff | Pyrite, smectite, chlorite |
| 630 | 632 | Same but with minor calcite. | Acid tuff | Pyrite, calcite, smect., chlorite |
| 632 | 638 | Same but highly altered and fractured. | Acid tuff | Pyrite, calcite, smect., chlorite |
| 638 | 640 | Same but abundant in dark grey cuttings (mixed cuttings of tuff and basalt) | Acid tuff | Pyrite, calcite, smect., chlorite |
| 640 | 642 | Earth brown to grey, fine-grained rock, highly oxidised to brown. | Basalt | Pyrite, calcite, chlorite, oxides |
| 642 | 644 | Dark grey, slightly oxidised with micro veins infilled with silica. Mixed cuttings of both tuff and basalt. | Basalt | Pyrite, calcite, chalcedony |
| 644 | 650 | Same | Basalt | Pyrite, calcite, chlorite |
| 650 | 662 | Loss of circulation returns | | |
| 662 | 664 | Dark grey to brownish, fine grained with veins infilled by calcite. | Basalt | Pyrite, calcite, chlorite |
| 664 | 676 | Same | Basalt | Pyrite, calcite, chlorite |
| 676 | 678 | Light grey to green, fine-grained tuffaceous material. Highly fractured with fresh epidote noted. It has mixed cuttings of basaltic formation. | Acid tuff | Chlorite, pyrite, epidote, quartz calcite |
| 678 | 680 | Same but with abundant basaltic material. | Acid tuff | Epidote, chlori., illite, pyrite, quartz, calcite |
| 680 | 684 | Same | Acid tuff | Epidote, chlori., pyrite, quartz |
| 684 | 690 | Light grey fine-grained fractured mixed cuttings of tuff and trachytes. Secondary quartz is discerned with epidote growing on top. Relatively porous w. veins infilled w. clays | Acid tuff | Chlorite, epidote, quartz calcite |
| 690 | 696 | Grey, fine-grained slightly oxidized rock with mixed cuttings of trachyte and tuffaceous materials | Acid tuff | Chlorite, epid., quartz calcite, oxides |
| 696 | 698 | Loss of circulation returns | | |
| 698 | 700 | Grey, fine-grained slightly oxidized rock with mixed cuttings of trachyte and tuffaceous materials | Trachytic tuff | Chlorite |
| 700 | 702 | Same | Trachytic tuff | Chlorite |
| 702 | 704 | Same | Trachytic tuff | Chlorite |
| 704 | 706 | Same | Trachytic tuff | Chlorite |
| 706 | 708 | Loss of circulation returns | | |
| 708 | 710 | Same | | Chlorite |
| 710 | 712 | Grey, fine-grained slightly oxidized rock with mixed cuttings of trachyte and tuffaceous materials | Trachytic tuff | Chlorite |

| Top (m) | Base (m) | Rock description | Rock type | Secondary minerals |
|---|---|---|---|---|
| 712 | 714 | Same | Trachytic tuff | Chlorite |
| 714 | 716 | Same | Trachytic tuff | Chlorite |
| 716 | 718 | Variant composition of grey and green trachytic rock fragments with some tuffaceous materials. Feldspar porphyrites are discerned in the rock matrix and pores which are infilled with felsic minerals are observed | Trachyte | Calcite, epidote, chlorite |
| 718 | 726 | Light grey fine-grained homogeneous rock | Trachyte | Calcite, epidote, chlorite, pyrite |
| 726 | 732 | Same | Trachyte | Chalcopyrite, quartz, chlorite |
| 732 | 740 | Dull green fine-grained moderately vesicular rock with some mixed cuttings of non-crystalline tuffaceous materials | Trachyte | Epidote, chlorite, illite, pyrite |
| 740 | 742 | Greyish to brown fine-grained slightly porous rock infilled with felsic minerals (silica) | Trachyte | Epidote, chlori., illite, pyrite |
| 742 | 744 | Loss of circulation returns | | |
| 744 | 748 | Light grey to green, fine-grained rock. It is vesicular with lithic materials and shows high intensity of alteration | Trachyte | Epidote, chlori., illite, pyrite |
| 748 | 750 | Dull brown to grey, fine-grained crystalline rock with mixed cuttings of tuffaceous material. It is highly altered and moderately oxidized | Trachyte | Epidote, chlori., illite, pyrite, calcite |
| 750 | 754 | Same; but with no calcite | Trachyte | Epidote, chlori., illite, pyrite |
| 754 | 756 | Loss of circulation returns | | |
| 756 | 760 | Dull brown to grey, fine-grained crystalline rock with mixed cuttings of tuffaceous material. It is highly altered and moderately oxidized | Trachyte | Epidote, chlorite, illite, pyrite |
| 760 | 764 | Greyish, fine-grained crystalline rock, it has laths of feldspar phenocrysts stained with oxides | Trachyte | Epidote, chlori., illite, pyrite |
| 764 | 766 | Dull grey to brown with white matrix of silica and laths of feldspars that have been altered to brown and green clays. it shows pores infilled with quartz and feldspar minerals | Trachyte | Epidote, chlorite, illite, pyrite, calcite |
| 766 | 770 | Light grey, fine-grained with mixed cuttings of crystalline minerals not well developed. Moderate to highly altered with pores infilled with feldspars and quartz | Trachyte | Epidote, chlori., illite, chalcopy, calcite |
| 770 | 784 | Loss of circulation returns | | |
| 784 | 788 | Dull grey, fine grained slightly to moderately altered. It has fragmented cuttings of tuffaceous materials. It is fractured with vein filled with quartz and feldspars | Trachyte | Epidote, chlorite, illite, pyrite |
| 788 | 794 | Same | Trachyte | Epidote, chlori., illite, chalcopy., calcite |
| 794 | 802 | Same | Trachyte | Pyrite, chlorite, illite, calcite |
| 802 | 808 | Same | Trachyte | Chlorite, illite |
| 808 | 812 | Same | Trachyte | Calcite, chlorite, illite |

| Top (m) | Base (m) | Rock description | Rock type | Secondary minerals |
|---|---|---|---|---|
| 812 | 820 | Same | Trachyte | Chlorite, illite |
| 820 | 828 | Greyish to brown, fine grained moderately altered with some phenocrysts of feldspar laths | Trachyte | Pyrite, chalcop., epidote, calcite, hematite, sideri., chlorite |
| 828 | 832 | Same; but the felsic minerals are fine grained and the rock is moderately fractured | Trachyte | Pyrite, quartz, siderite, calcite, chalcop., chlori. |
| 832 | 834 | Light grey fine-grained homogenous rock with high intensity of alteration | Trachyte | Pyrite, chalcop., chlorite, calcite |
| 834 | 836 | Greyish to brown, fine grained moderately altered with some phenocrysts of feldspar laths | Trachyte | Pyrite, quartz, siderite, calcite, chalcop., chlori. |
| 836 | 848 | Same; with phenocrysts of feldspar laths | Trachyte | Pyrite, siderite, calcite, chlorite |
| 848 | 854 | Same; but highly altered rock to clays and oxidized (generally greyish) | Trachyte | Pyrite, siderite, calcite, chlorite |
| 854 | 856 | Greyish, fine-grained, slightly to moderately altered rock with phenocrysts of feldspar laths. Shows moderate intensity of oxidation. The rock is also fractured | Trachyte | Chalcopyrite, pyrite, calcite, chlorite |
| 856 | 860 | Same; but the felsic minerals are more abundant | Trachyte | Chalcop., pyrite, calcite, chlorite |
| 860 | 880 | Same; but dull grey to brown | Trachyte | Chalcop., pyrite, calcite, chlorite |
| 880 | 882 | Same; but medium grained and appears fractured | Trachyte | Chalcop., pyrite, calcite, chlorite |
| 882 | 884 | Same; Light grey in colour | Trachyte | Chalcop., pyrite, calcite, chlorite |
| 884 | 886 | Same; But dark to dull grey in colour | Trachyte | Chalcop., pyrite, calcite, chlorite |
| 886 | 894 | Same; and shows flow texture with NO calcite | Trachyte | Chalcop., pyrite, chlorite |
| 894 | 896 | Same and shows moderate alteration | Trachyte | Chalcopyrite, pyrite, chlorite |
| 896 | 898 | Same, with little calcite | Trachyte | Chalcop., pyrite, calcite, chlorite |
| 898 | 910 | Grey, fine-grained, moderately altered rock with phenocrysts laths of feldspar. Slightly oxidized on occasional grains | Trachyte | Chalcopyrite, pyrite, calcite, chlorite |
| 910 | 914 | Same; with tiny pyrite disseminations | Trachyte | Chalcop., pyrite, calcite, chlorite |
| 914 | 930 | Same; greyish to light grey, fine-grained porphyritic rock with laths of feldspars. Moderately altered | Trachyte | Pyrite, chalcop., chlorite |
| 930 | 950 | Same; but dull grey with little calcite | Trachyte | Pyrite, chalcop., chlorite, quartz, calcite |
| 950 | 952 | Same; but dark grey to brown | Trachyte | Calcite, epidote, pyrite, chlorite |
| 952 | 962 | Same | Trachyte | Pyrite, calcite, |

| Top (m) | Base (m) | Rock description | Rock type | Secondary minerals |
|---|---|---|---|---|
| | | | | chlorite |
| 962 | 974 | Same | Trachyte | Pyrite, chlorite |
| 974 | 980 | Same; but greyish green in colour | Trachyte | Chlorite, illite |
| 980 | 982 | Dull brown to grey, fine-grained crystalline rock. Moderately altered to green and brown clays | Rhyolite | Calcite, pyrite, epidote, chlorite |
| 982 | 984 | Same | Rhyolite | Calcite, pyrite, epidote, chlorite |
| 984 | 992 | Earth grey, fine-grained cryptocrystalline rock and slightly altered to occasional clays | Rhyolite | Pyrite, chlorite |
| 992 | 994 | Grey, fine-grained moderately altered to green rock with clearly discernible feldspar laths | Trachyte | Epidote, chalcop., pyrite, prehnite, chlori. |
| 994 | 1000 | Same; but more oxidized | Trachyte | Epidote, chalcop., pyrite, prehni., chlorite |
| 1000 | 1006 | Light grey to dull, fine-grained rock. moderately oxidized with laths of feldspars | Trachyte | Pyrite, epidote, chlorite |
| 1006 | 1008 | Greyish to green, fine-grained rock. Highly altered to clays | Trachyte | Chlorite, pyrite, epido., chalcop. |
| 1008 | 1016 | Grey, fine-grained rock with anhedral feldspar crystals. Highly altered to clays | Trachyte | Chlorite, pyrite, epido., chalcop. |
| 1016 | 1020 | Brown; fine-grained rock, highly oxidized to brown clays with high intensity of alteration | Rhyolite | Chlorite, illite, pyrite, epidote, chalcopyrite |
| 1020 | 1022 | Same but highly oxidized | Rhyolite | Chlorite, illite, pyrite |
| 1022 | 1028 | Grey, fine-grained slightly to moderately oxidized rock. It is flaky and compact with sporadic pores | Rhyolite | Chalcop., pyrite, chlorite, illite |
| 1028 | 1030 | Light grey, fine-grained rock with phenocrysts of feldspars. Moderately altered | Trachyte | Epidote, pyrite, chalcopyrite, chlorite, illite |
| 1030 | 1044 | Same; but more felsic with some pyroxene. Also abundant clays and epidote is noted | Trachyte | Epidote, chlori., illite, pyrite |
| 1044 | 1046 | Dull grey with highly altered feldspar phenocrysts. Highly oxidized to brown. | Trachyte | Calcite, chlorite, illite |
| 1046 | 1048 | Same | Trachyte | Calcite, chlorite, illite |
| 1048 | 1068 | Dull green rock with highly altered feldspar phenocrysts. Slightly oxidized to brown clays | Trachyte | Pyrite, chlorite, illite, oxides |
| 1068 | 1070 | Light grey, fine grained slightly oxidized and moderately altered | Trachyte | Pyrite, chalcop., chlorite, illite |
| 1070 | 1078 | Same; with little oxidation | Trachyte | Pyrite, chalcop., chlorite, illite |
| 1078 | 1088 | Same; Light to dark grey, moderately altered rock with abudant feldspars | Trachyte | Pyrite, chalcop., chlorite, illite |
| 1088 | 1094 | Grey, moderately porphyritic rock with white feldspars, moderately altered to brown and green clays in a fine-grained matrix (feldspar laths are discerned) | Trachyte | Pyrite, chalcop., chlorite, illite, oxides |
| 1094 | 1096 | Light grey fine-grained, highly altered rock into clays. It is | Trachyte | Pyrite, chlorite, |

| Top (m) | Base (m) | Rock description | Rock type | Secondary minerals |
|---|---|---|---|---|
| | | homogenous with slight oxidation state | | illite, oxides |
| 1096 | 1098 | Grey, moderately porphyritic rock with white feldspar lath. Moderately altered to brown and green clays | Trachyte | Chlorite, illite, pyrite, chalcop., oxides |
| 1098 | 1104 | Same; but slightly altered and oxidized | Trachyte | Chlorite, illite, pyrite, oxides, calcite |
| 1104 | 1110 | Same | Trachyte | Chlorite, illite, pyrite |
| 1110 | 1114 | Grey, fine grained, slightly altered and shows slight intensity of oxidation. | Trachyte | Epidote, chlori., illite, pyrite |
| 1114 | 1118 | Greyish, brown, fine grained with phenocrysts of feldspar laths. slightly oxidised. | Trachyte | Chlorite, illite, pyrite |
| 1118 | 1124 | Same, but moderately altered. | Trachyte | Chlorite, illite, oxides, pyrite |
| 1124 | 1132 | Same but slightly to moderately altered with abundance of clay minerals. | Trachyte | Chlorite, illite, oxides, pyrite |
| 1132 | 1134 | Earth brown, fine-grained, slightly porphyritic rock. it highly oxidised and altered. | Trachyte | Chlorite, illite, oxides, pyrite |
| 1134 | 1136 | Same but with mixed cuttings of light grey fragments. | Trachyte | Chlorite, illite, oxides, pyrite |
| 1136 | 1142 | Light grey, fine-grained, highly altered rock and slightly oxidised. | Trachyte | Chlorite, illite |
| 1142 | 1144 | Same but moderately altered with vein infilled with pyrite. | Trachyte | Chlorite, illite |
| 1144 | 1146 | Same but slightly fractured. | Trachyte | Chlorite, illite, pyrite |
| 1146 | 1152 | Light grey to green, fine-grained, moderately altered rock. | Trachyte | Chlorite, illite |
| 1152 | 1154 | Same but with mixed cuttings of a darker grey lava | Trachyte | Chlorite, illite, oxides |
| 1154 | 1170 | Grey, moderately altered rock with quartz phenocrysts. Slightly oxidised. | Trachyte | Chlorite, illite, pyrite |
| 1170 | 1172 | Light grey, relatively fresh and feldspar rich lava. slightly altered to green clays. | Trachyte | Calcite, chlorite, illite, pyrite |
| 1172 | 1176 | Dark grey to brown, fine-grained, poorly porphyritic, moderately altered to brown clays. | Basalt | Chlorite, illite, calcite, epidote, quartz, pyrite |
| 1176 | 1180 | Same but with calcite | Basalt | Chlorite, illite, calcite, epidote, quartz, pyrite |
| 1180 | 1200 | Same but with no calcite | Basalt | Chlorite, illite, epidote, pyrite |
| 1200 | 1208 | Light grey, fine grained, highly altered with mixed cuttings of basaltic composition. | Trachyte | Chlorite, illite |
| 1208 | 1210 | Same but moderately altered with phenocrysts of feldspar laths. | Trachyte | Chlorite, illite, oxides |
| 1210 | 1212 | Grey to brown, fine-grained rock; weakly porphyritic, moderately oxidised to oxides and clays. | Basalt | Pyrite, oxides, chlorite, illite |
| 1212 | 1214 | Same but with mixed cuttings of trachytic formation. | Basalt | Chlorite, illite, oxides |

| Top (m) | Base (m) | Rock description | Rock type | Secondary minerals |
|---|---|---|---|---|
| 1214 | 1216 | Same | Basalt | Pyrite, oxides, chlorite, illite |
| 1216 | 1218 | Same | Basalt | Pyrite, chlorite, illite |
| 1218 | 1220 | Grey, fine grained, with some feldspar laths (weakly porphyritic). Moderately altered to clays and shows slight intensity of alteration. | Basalt | Pyrite, chlorite, illite |
| 1220 | 1222 | Same but fractured | Basalt | Pyrite, chlorite, illite |
| 1222 | 1224 | Same | Basalt | Pyrite, wairak., chlorite, illite |
| 1224 | 1226 | Same | Basalt | Chlorite, illite, pyrite, quartz |
| 1226 | 1228 | Greyish to brownish, fine-grained weakly porphyritic rock. it is moderately altered with mixed cuttings of basaltic formation. | Trachyte | Chlorite, illite, pyrite, quartz |
| 1228 | 1232 | Same but lightly greyish with slight intensity of alteration. The rock is slightly porous. | Trachyte | Chlorite, illite, pyrite, oxides |
| 1232 | 1234 | Same but with mixed cuttings of basaltic formation. | Trachyte | Prehnite, chlori., illite, pyrite, oxides, wairak. |
| 1234 | 1238 | Same | Trachyte | Chlorite, illite, pyrite, oxides, prehnite |
| 1238 | 1244 | Greyish to brownish, fine-grained with slight phenocrysts of feldspar laths. moderately altered and oxidised rock. | Basalt | Pyrite, chlorite, illite, oxides |
| 1244 | 1246 | Same but slightly to moderately altered and slightly oxidised. | Basalt | Calcite, chlorite, illite |
| 1246 | 1248 | Same but with mixed cuttings of trachytic formation. | Basalt | Calcite, chlorite, illite |
| 1248 | 1256 | Grey to brownish, fine grained, slightly to moderately altered to clays. | Basalt | Pyrite, chlorite, illite, oxides |
| 1256 | 1258 | Greyish to brownish, fine grained, moderately porphyritic and moderately altered and oxidised. | Trachyte | Chlorite, illite, oxides, quartz |
| 1258 | 1276 | Same but the abundance of secondary quartz, the rock is relatively vesicular infilled with secondary quartz. | Trachyte | Chlorite, illite, quartz, pyrite, fluorite |
| 1276 | 1278 | Green and grey, moderately porphyritic, feldspar rich rock. Highly altered to green and brown. Veins infilled | Trachyte | Pyrite, chlorite, illite, oxides, quartz |
| 1278 | 1280 | Same | Trachyte | Pyrite, chlorite, illite, oxides, quartz |
| 1280 | 1294 | Same but cuttings are small grains | Trachyte | Epidote, pyrite, chlorite, illite, quartz |
| 1294 | 1298 | Dark grey, fine-grained rock with poorly formed crystals of olivine?, pyroxene? mixed cuttings of the latter altered trachyte | Basalt | Pyrite, chalcopyrite, chlorite, illite |

| Top (m) | Base (m) | Rock description | Rock type | Secondary minerals |
|---|---|---|---|---|
| 1298 | 1300 | Dark grey, fine-grained rock with poorly formed crystals of olivine. Mixed with the latter altered trachytes. | Basalt | Pyrite, chalcop., chlorite, illite |
| 1300 | 1312 | Same but more oxidised. | Basalt | Pyrite, chalcop., chlorite, illite, calcite |
| 1312 | 1318 | Light grey, medium-grained rock with feldspar phenocrysts. Slightly altered to green and brown clays. Micro veins infilled with dark minerals. Scoria also identified. | Trachyte | Oxides, epidote, chlorite, illite |
| 1318 | 1342 | Mixed cuttings of green, light grey and brown colour, poorly sorted. Trachytic composition noted. Non crystalline altered tuffs also abundant. | Trachytic tuff | Pyrite, chalcop., wairak., hemati., oxides, chlorite, illite |
| 1342 | 1360 | Mixed cuttings of highly altered trachyte and tuff. Moderately oxidised. | Trachytic tuff | Chalcop., quartz oxides, pyrite, chlorite, illite |
| 1360 | 1366 | Light brown, feldspar rich lava with medium grains of felsic and mafic minerals. Highly altered. | Trachyte | Chlorite, illite, pyrite, oxides, epid., chalcop., quartz |
| 1366 | 1394 | Light green and grey, medium-grained rock with feldspar porphyrites. Moderately altered to green and brown clays. | Trachyte | Pyrite, chalcop., chlorite, illite, oxides, quartz |
| 1394 | 1406 | Light grey to green felsic rock with feldspar phenocrysts. Medium to fine grained and highly altered to green and brown clays. | Trachyte | Chlorite, illite, pyrite, hematite, quartz |
| 1406 | 1416 | Same but less altered. | Trachyte | Chlorite, illite, pyrite, oxides |
| 1416 | 1418 | Dark grey, moderately porphyritic, with feldspars phenocrysts. Slightly altered to brown clays. | Trachyte | Chlorite, illite, pyrite, oxides |
| 1418 | 1422 | Same but moderately altered. | Trachyte | Pyrite, chalcop., chlorite, illite, oxides |
| 1422 | 1434 | Light grey, moderately porphyritic feldspar rich rock with medium-grained pyroxenes, moderately altered to brown and green clays. Moderately oxidised. | Trachyte | Oxides, chalcop. chlorite, illite, quartz, pyrite |
| 1434 | 1442 | Same but less oxidised. | Trachyte | Oxides, quartz, pyrite, chlorite, illite, chalcop. |
| 1442 | 1456 | Same | Trachyte | Epidote, prehni., oxides, chlorite, illite, quartz, pyrite |
| 1456 | 1500 | Light grey, fine-grained, slightly porphyritic rock (porphyrites of haematite). Moderately altered. | Trachyte | Pyrite, hematite, prehni., sphene. chlorite, illite |
| 1500 | 1510 | Light grey fine-grained non-porphyritic rock composed of feldspar in the matrix. It is weakly altered to clays and anhedral mafic minerals noted in the matrix. | Trachyte | Chlorite, illite, epidote |
| 1510 | 1516 | Light grey fine-grained weakly porphyritic rock composed | Trachyte | Chlorite, illite, |

| Top (m) | Base (m) | Rock description | Rock type | Secondary minerals |
|---|---|---|---|---|
| | | of sanidine phenocrysts. It is weakly altered to clays and tiny pyrite is disseminated in the matrix. | | quartz epidote |
| 1516 | 1528 | Brownish grey fine grained composed of feldspar in the matrix. Veinlets are infilled by mafic minerals. | Trachyte | Chlorite, illite, pyrite epidote |
| 1528 | 1540 | Light grey fine-grained weakly porphyritic rock composed of euhedral to sub-hedral sanidine phenocrysts. Specs of mafic mineral also noted in the matrix. The formation is fractured and veins infilled by secondary quartz. Specs of mafic mineral that are being altered to sphene are noted. The formation is slightly oxidised, weakly altered to clays and tiny pyrite is disseminated in the matrix. | Trachyte | Chlorite, illite, pyrite, sphene quartz epidote |
| 1540 | 1552 | Greenish grey to brownish grey fine-grained and non-porphyritic rock composed of abundant feldspar in the matrix. The formation is fractured with veinlets infilled by clays and iron oxides. It is weakly altered to clays. Pyrite is disseminated in the matrix. | Trachyte | Sphene chlorite, illite, epidote |
| 1552 | 1554 | Grey to greenish grey fine-grained non-porphyritic rock. It is composed of feldspar in the matrix and anhedral mafic mineral in the groundmass. Weakly altered to fine green clays infilling vesicles. | Trachyte | Chlorite, illite, sphene epidote |
| 1554 | 1568 | Light grey to greenish grey fine grained composed of quartz and feldspar. Specs of mafic mineral noted and the formation is weakly altered to green clays infilling vesicles. | Rhyolitic tuff | Chlorite, illite, sphene epidote |
| 1568 | 1572 | Greenish grey fine-grained non-porphyritic rock. The formation is fractured w and veins and veinlets filled by pyrite and clays. At depth 1572-1574 m, epidote is precipitated in veins and vesicles. The formation is moderately altered. | Tuff | Sphene, epidote, chlorite, illite |
| 1572 | 1582 | Light grey fine-grained non-porphyritic rock. Occasional cryptocrystalline fragments are noted. The formation is fractured and veinlets infilled by clays. It is weakly altered to clays and moderately oxidised. | Rhyolite | Chlorite, illite, epidote, pyrite |
| 1582 | 1600 | Light grey fine-grained weakly porphyritic rock composed of abundant feldspar and phenocrysts of quartz. It is fractured and veins and veinlets infilled by clays, mafic mineral and secondary quartz. The formation is weak to moderately altered to clays. | Trachyte | Quartz, chlorite, illite, sphene, epidote, pyrite |
| 1600 | 1606 | Greenish grey to light grey fine-grained non-porphyritic rock. Euhedral to subhedral magnetite is noted in the matrix and the formation is weakly altered, slightly fractured and veinlets infilled by felsic mineral. | Trachyte | Sphene, chlorite, illite, epidote |
| 1606 | 1618 | Grey fine-grained non-porphyritic rock. It is fractured and veins infilled by secondary quartz, epidote and pyrite. | Trachyte | Quartz, epidote, chlorite, illite, sphene |
| 1618 | 1634 | White to light grey fine- to medium-grained rock composed of quartz and feldspar. Specs of mafic mineral are noted in the matrix. The formation is weakly altered to clays and fractured and veins infilled by mafic mineral. | Trachyte | Chlorite, illite, sphene, epidote, actinolite |
| 1634 | 1642 | Grey fine-grained weakly porphyritic rock composed of euhedral sanidine and feldspar. It is fractured and epidote | Trachyte | Epidote chlorite, illite, quartz, |

| Top (m) | Base (m) | Rock description | Rock type | Secondary minerals |
|---|---|---|---|---|
| | | and quartz are precipitated in veins. The formation is moderately altered to clays infilling vesicles. Wairakite is noted at depth 1644-1646 m. | | hematite, sphene |
| 1642 | 1662 | Light grey fine-grained non-porphyritic rock composed of quartz and feldspar in the groundmass. Euhedral to subhedral magnetite altering to hematite is also noted. The formation is slightly oxidised and weakly altered to clays. | Rhyolite | Chlorite, illite, hematite, epidote |
| 1662 | 1668 | Grey fine-grained non-porphyritic rock composed of laths of feldspar. The formation is weakly altered to clays. | Trachyte | Chlorite, illite, epidote |
| 1668 | 1678 | Greyish brown fine-grained weakly porphyritic and heterogeneous rock comprising of trachyte, tuff and rhyolite. It is fractured and veinlets infilled by mafic minerals. The formation is weakly altered. | Tuff | Chlorite, illite, pyrite, epidote |
| 1678 | 1686 | Loss of circulation returns | | |
| 1686 | 1744 | Grey fine-grained and weakly porphyritic rock composed of anhedral sanidine in the matrix. It is fractured and veins infilled by quartz and green clays. The formation is weakly altered to clays and slightly oxidised. | Trachyte | Quartz, chlorite, illite, epidote |
| 1744 | 1750 | Greyish brown fine-grained and weakly porphyritic rock composed of sanidine in the matrix. It is fractured and veins infilled by epidote and mafic mineral. Epidote is also precipitated on the rock surfaces. It is moderately oxidised and weak to moderately altered to green clays. | Trachyte | Hematite chlorite, illite, epidote, quartz |
| 1750 | 1752 | Loss of circulation return | | |
| 1752 | 1814 | Grey fine-grained and weakly porphyritic rock composed of quartz and feldspar in the matrix. It is moderately altered to green clays. | Rhyolite | Chlorite, illite, epidote |
| 1814 | 1872 | Light grey fine- to medium-grained moderately porphyritic rock composed of quartz and feldspar. It is fractured with veins filled by clays and moderately altered to clays. | Trachyte | Chlorite, illite, epidote, quartz |
| 1872 | 1876 | Loss of circulation return | | |
| 1876 | 2010 | Light grey fine- to medium-grained moderately porphyritic rock composed of quartz and feldspar. It is fractured with veins filled by clays and moderately altered to clays. | Trachyte | Sphene, chlorite, illite, pyrite |
| 2010 | 2018 | Same but with increasing oxidation. | Trachyte | Sphene, chlori., illite, pyrite |
| 2018 | 2028 | Greyish, fine- to medium-grained, weakly porphyritic rock, slightly vesicular with fine-grained clays infilling the vesicles. Appears dense or massive. | Trachyte | Sphene, chlorit., illite, pyrite, chalcopyrite |
| 2028 | 2030 | Same but with increased oxidation. | Trachyte | Sphene, chlorit., illite, pyrite, chalcopyrite |
| 2030 | 2042 | Same but with increased pyrite dissemination in the matrix. | Trachyte | Epidote, sphene, chlorite, illite, pyrite |
| 2042 | 2046 | Same but with calcite. | Trachyte | Epidote, sphene, chlorite, illite, pyrite, calcite |
| 2046 | 2050 | Same but greenish to greyish, with fine to medium grains | Trachyte | Epidote, sphene, |

| Top (m) | Base (m) | Rock description | Rock type | Secondary minerals |
|---|---|---|---|---|
| | | | | chlorite, illite, pyrite, calcite |
| 2050 | 2058 | Greyish brown, fine-grained rock, slightly porphyritic with subhedral laths of feldspars. Finely disseminated pyrite is observed in the matrix. | Trachyte | Pyrite, chlorite, illite, epidote, chalcop., hemat. |
| 2058 | 2060 | Same but with increased abundance of felsic minerals (feldspars) | Trachyte | Pyrite, chlorite, illite, epidote, chalcop., hemat. |
| 2060 | 2062 | Same; traces of biotite noted? | Trachyte | Wollast., pyrite, chlorite, illite, hemat., chalcop. |
| 2062 | 2068 | Same | Trachyte | Wollast., pyrite, chlorite, illite, hemat., chalcop. |
| 2068 | 2100 | Same but with increased oxidation. | Trachyte | Wollast., pyrite, chlorite, illite, hemat., chalcop. |
| 2100 | 2106 | Light grey to brownish, fine-grained rock. It is weakly porphyritic with sporadic euhedral laths of Sanidine. moderately oxidised and altered. Vein infilled with felsic minerals are noted. | Trachyte | Pyrite, chalcop., chlorite, illite, hematite, quartz |
| 2106 | 2116 | Same but highly oxidised | Trachyte | Pyrite, chalcop., chlorite, illite, hematite, quartz, magnetite |
| 2116 | 2120 | Same but fractured and heterogeneous rock. | Trachyte | Epidote, pyrite, chalcop., chlori., illite, hematite |
| 2120 | 2134 | Same but highly fractured and vesicular (infilled with magnetite). Heterogeneous rock | Trachyte | Epidote, pyrite, chalcop., chlori., illite, hematite |
| 2134 | 2142 | Brownish to greenish, fine grained and heterogeneous. | Tuff | Pyrite, chalcop., chlorite, illite, hematite |
| 2142 | 2154 | Greenish, grey to dull brown, fine- to medium-grained rock. it appears slightly altered to green clays. Occasional phenocrysts of feldspar laths visible in the matrix and tiny pyrite disseminations in the matrix are observed. | Trachyte | Chlorite, illite, pyrite |
| 2154 | 2160 | Same but dull grey, fine to medium grained, traces of actinolite are noted. | Trachyte | Actinol., pyrite, chlorite, illite |
| 2160 | 2164 | Same but with increased pyrite. | Trachyte | Actinol., pyrite, chlorite, illite |
| 2164 | 2170 | Greyish brown, fine-grained rock, with sporadic pheno-crysts laths of sanidine. Moderately oxidised with slight alteration micro veins infilled with felsic minerals noted. | Trachyte | Hematite, illite, pyrite, chlorite |
| 2170 | 2172 | Same but more dull. | Trachyte | Hematite, illite, pyrite, chlorite |
| 2172 | 2180 | Same but more altered to clays (chlorite). | Trachyte | Hematite, illite, pyrite, chlorite |

| Top (m) | Base (m) | Rock description | Rock type | Secondary minerals |
|---|---|---|---|---|
| 2180 | 2184 | Same but light grey with slight alteration. | Trachyte | Hematite, illite, pyrite, chlorite |
| 2184 | 2190 | Dull grey, fine- to medium-grained rock. Moderately altered to clays and slightly oxidised. | Trachyte | Quartz, clays, chlorite, illite, pyrite, hematite |
| 2190 | 2198 | Same but the rock appears light grey, with most of the pyroxenes being replaced by clays. | Trachyte | Quartz, chlorite, illite, pyrite, hematite |
| 2198 | 2204 | Same but with increased secondary quarts pyrite. | Trachyte | Quartz, pyrite, actinolite, chlorite, illite |
| 2204 | 2232 | White, coarse to medium-grained highly felsic rock (rich in silica). It is moderately to highly altered with foreign trachyte fragments. | Rhyolitic intrusion | Quartz, actinol., chlorite, illite, pyrite |
| 2232 | 2234 | White to light grey, fine- to medium-grained, weakly porphyritic rock, with mixed fragments of rhyolitic composition. | Rhyolitic intrusion | Hemat., actinol., chlorite, illite, pyrite |
| 2234 | 2248 | Light grey, fine- to medium-grained, poorly porphyritic rock with fragments spotted with oxides. Moderately altered with slight oxidation. | Trachyte | Actinolite, chlorite, illite, pyrite |
| 2248 | 2250 | Dull grey, fine- to medium-grained, weakly porphyritic rock. Occasional phenocrysts of sanidine laths discerned and appears slightly altered. It shows mild flow texture. | Trachyte | Chlorite, illite |
| 2250 | 2260 | Light grey, fine to medium grained, weakly porphyritic with spotted mafics and oxides. They have pyrite disseminations that occur sporadically. | Trachyte | Actinolite, chlorite, illite, pyrite |
| 2260 | 2264 | Dull grey, fine- to medium-grained rock. It is moderately altered to green clays. Tiny pyrite disseminations are also noted in the groundmass. | Trachyte | Epidote, chlorite, illite, pyrite |
| 2264 | 2268 | Light grey, fine- to medium-grained rock. It appears slightly altered with tiny sporadic pyrite disseminations. | Trachyte | Actinol., chlori., illite, pyrite |
| 2268 | 2270 | Light grey, to reddish brown, fine-grained rock. Appears slightly altered to clays with sporadic tiny pyrite disseminations. | Trachyte | Chlorite, illite, quartz |
| 2270 | 2272 | Light grey, fine-grained, felsic rock with reddish brown specs of oxides. Minor occasional traces of actinolite noted. | Trachyte | Actinolite, chlorite, illite |
| 2272 | 2278 | Same but appears dull. | Trachyte | Actinolite, chlorite, illite |
| 2278 | 2286 | Light grey, dense and massive, fine-grained trachyte. Sanidine laths are observed as phenocrysts and sporadic specs of mafics. Slightly oxidised fragments are noted. | Trachyte | Actinolite, chlorite, illite, pyrite |
| 2286 | 2288 | Same but the oxidation increases. | Trachyte | Actinol., chlori., illite, pyrite |
| 2288 | 2290 | Same but with pyroxenes altered to amphiboles. | Trachyte | Actinol., chlori., illite, pyrite |
| 2290 | 2292 | Light to dark green, fine- to medium-grained, slightly porphyritic rock. Shows distinct trachytic texture and moderately porous. It is slightly fractured and increasing actinolite. | Trachyte | Actinolite, chlorite, illite. Pyrite |

| Top (m) | Base (m) | Rock description | Rock type | Secondary minerals |
|---|---|---|---|---|
| 2292 | 2294 | White to light grey, medium- to coarse-grained, moderately porphyritic rock. Slightly oxidised. Pyrite disseminated in matrix. | Syenite | Actinolite, chlorite, illite |
| 2294 | 2298 | Same | Syenite | Actinol., chlori., illite, pyrite |
| 2298 | 2318 | Light grey to light brown, fine- to medium-grained, moderately porphyritic rock. Slightly oxidised pyrite disseminations noted. | Trachyte | Actinolite, chlorite, illite. Pyrite |
| 2318 | 2320 | Grey fine- to medium-grained rock, moderately porphyritic, with quartz phenocrysts. Slightly fractured rock. | Trachyte | Chlorite, illite, quartz, calcite |
| 2320 | 2336 | Light grey, fine-grained, moderately porphyritic rock, with sporadic laths of feldspar phenocrysts. Slightly oxidised with traces of alteration to clays. | Trachyte | Illite, quartz, pyrite, chlorite |
| 2336 | 2340 | Grey, fine-grained rock, moderately altered to clays with occasional traces of epidote with slight oxidation. | Trachyte | Chlorite, illite, epidote |
| 2340 | 2342 | Light grey, medium-grained rock. Pyroxenes are discernible in the matrix and appear fresh, with slight oxidation. | Trachytic intrusion | Chlorite, illite |
| 2342 | 2344 | Same but with increased oxidation. | Trachytic intrusion | Chlorite, illite |
| 2344 | 2352 | Same | Trachyte | Chlorite, illite |
| 2352 | 2354 | Dull grey, fine-grained, poorly porphyritic rock, micro veins infilled with mafic minerals are noted, slightly oxidised but the rock appears generally fresh. | Trachyte | Calcite, chlorite, illite |
| 2354 | 2362 | Dull grey, fine-grained, moderately porphyritic, veins infilled with mafics. Slightly oxidised, mnor calcite noted. | Trachyte | Calcite, chlorite, illite |
| 2362 | 2368 | Light brown to grey, fine-grained, dense rock. Slightly porphyritic with clearly discernible feldspar laths, fractured. | Trachyte | Quartz, pyrite, chlorite, illite |
| 2368 | 2372 | Brown to light grey, fine grained. It has vesicles infilled with felsic minerals, with sporadic laths of feldspar phenocrysts. | Trachytic tuff | Actinolite, pyrite, chlorite, illite |
| 2372 | 2382 | Same but more tuffaceous fragments are incorporated in the matrix | Tuff | Actinol., pyrite, chlorite, illite |
| 2382 | 2394 | Brownish grey, fine-grained, highly porous rock with glassy texture. Euhedral crystals of feldspar laths appear as xenoliths in a fine-grained cryptocrystalline matrix. Tuffaceous fragments are highly oxidised. | Tuff | Epidote, chlorite, illite, hematite, actinolite |
| 2394 | 2396 | Same but with increased scoraceous material. | Tuff | Epid., chlorite, illite, hematite, actinol., pyrite, calcite |
| 2396 | 2398 | Same but with a lot of scoria. | Tuff | Epid., chlorite, illite, hematite, actinol., pyrite, calcite |
| 2398 | 2404 | Highly heterogeneous rock. | Tuff | Illite, chlorite, actinol., sphene, epidote, pyrite, hematite |
| 2404 | 2410 | Greyish green, fine-grained dense cryptocrystalline rock | Trachyte | Epid., chlorite, |

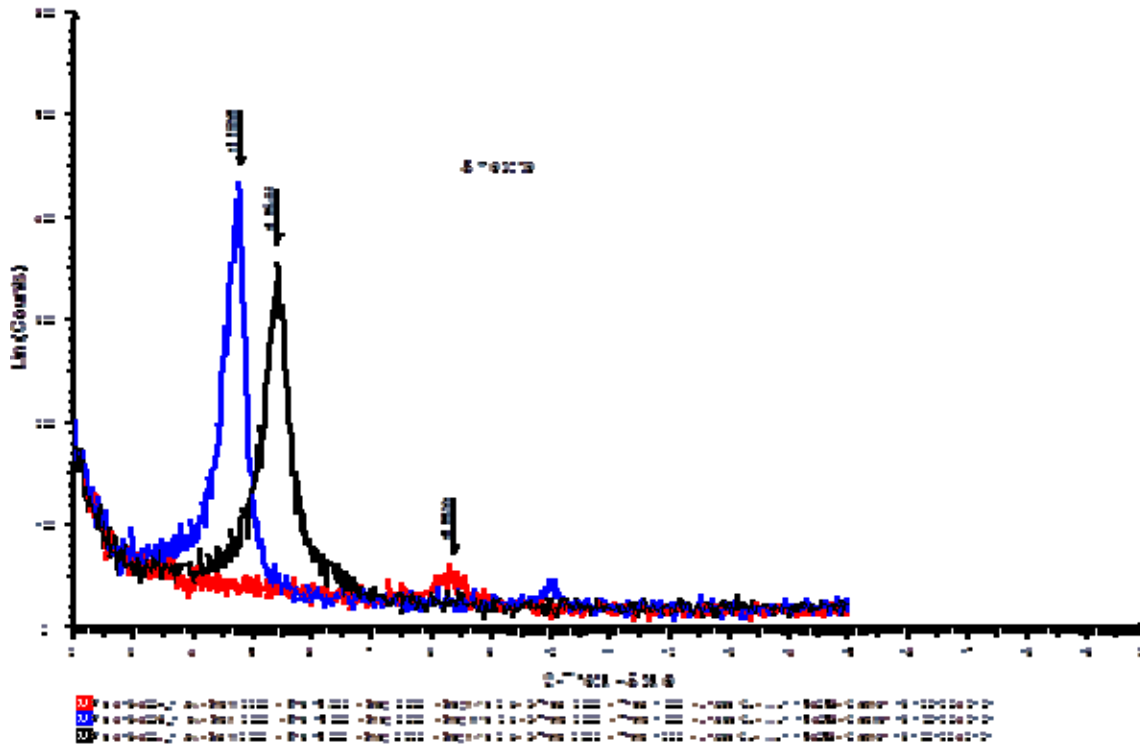| Top (m) | Base (m) | Rock description | Rock type | Secondary minerals |
|---|---|---|---|---|
| | | with occasionally incorporated fragments of tuffs. Vein filled with chlorite are also discerned. It is homogeneous and non-porphyritic rock. Slightly fractured. | | illite, actinolite, pyrite, hematite, sphene |
| 2410 | 2414 | Same but homogeneous and highly cryptocrystalline. | Trachyte | Epido., chlorite, illite, actinolite, pyrite, hematite, sphene. |
| 2414 | 2434 | Same | Trachyte | Epido., chlorite, illite, sphene, pyrite |
| 2434 | 2454 | Grey, fine-grained, cryptocrystalline, dense rock. Slightly fractured with moderate to slight alteration. Tiny pyrite disseminations noted in the groundmass. | Trachyte | Epidote, actinol., quartz, chlorite, illite |
| 2454 | 2464 | Same but the rock appears green to light grey with spotted mafic minerals. | Trachyte | Chlorite, illite, epidote, quartz, sphene |
| 2464 | 2468 | Light green, fine- to medium-grained trachyte. Discernible feldspar laths noted. It exhibits primary porosity infilled with clays/chlorites. It is highly altered to chlorite and occasional sphene. | Trachyte | Epidote, actinolite, chlorite, illite, sphene, pyrite |
| 2468 | 2470 | Same but appears more fractured and moderately oxidised. | Trachyte | Epidote, actinolite, chlorite, illite, sphene, pyrite |
| 2470 | 2488 | Same but with reduced oxidation. | Trachyte | Epido, actinol., chlorite, illite, sphene, pyrite |
| 2488 | 2500 | Same and highly altered rock with clear epidote. | Trachyte | Epidote, chlorite, illite, sphene, pyrite |
| 2500 | 2504 | Dark grey, fine-grained, feldspar (sanidine) rich porphyrites. Massive, moderately altered, epidote crystals observed, sphene. | Trachyte | Epidote, sphene, magnetite, chlorite, illite, |
| 2504 | 2510 | Same but slightly oxidised. | Trachyte | Epidote, sphene, magnetite, chlorite, illite, |
| 2510 | 2540 | Mixed cuttings of dark grey, basaltic lava and light grey, feldspar and pyroxene rich rhyolite lava. Basaltic fragments. Slightly oxidised. Brown and green clays noted. | Basalt | Epidote, sphene, chlorite, illite |
| 2540 | 2542 | Same | Rhyolite | Illite, chlorite, epidote |
| 2542 | 2548 | Same but with micro veins. Highly oxidised. | Basalt | Illite, chlorite, epidote |
| 2548 | 2552 | Light grey, felsic, with sanidine and quartz phenocrysts. Medium-grained, slightly altered and massive textured rock. Pyroxenes also visible. | Rhyolite | Illite, chlorite, epidote |
| 2552 | 2564 | Black to greenish, grey, fine- and medium-grained basaltic lava. Moderately altered. Abundant mafic minerals. | Basalt | Chlorite, illite, hemati., sphene, actinolite |

| Top (m) | Base (m) | Rock description | Rock type | Secondary minerals |
|---|---|---|---|---|
| 2564 | 2570 | Loss of circulation | | |
| 2570 | 2604 | Light grey, medium-grained, subhedral rock. Subhedral feldspars and mafics observed. Slightly altered to green and brown. | Trachyte | Chlorite, illite, hemati., sphene, actinoli., epidote |
| 2604 | 2614 | Loss of circulation | | |
| 2614 | 2634 | Light grey, fine- to medium-grained felsic rock. Shows flow texture. Slightly altered to green and brown clays and oxides. Micro veins noted. | Trachyte | Illite, epidote, hematite, actinolite |
| 2634 | 2648 | Loss of circulation | | |
| 2648 | 2668 | Light grey to green, fine-grained matrix, with subhedral sanidine phenocrysts. Slightly altered to green clays. Slightly oxidised. Sanidine being replaced by chlorites. | Trachyte | Illite, epidote |
| 2668 | 2674 | Loss of circulation | | |
| 2674 | 2712 | Light grey to green, fine-grained, felsic rock. Moderately altered to green clay. Brown illite also noted. Slight oxidation noted. | Trachyte | Epidote, illite, sphene |
| 2712 | 2726 | Mixed cuttings of grey trachytic rock with brown clastic fragments. Clastics highly oxidised. | Scoria | Chlorite, epido., illite, sphene |
| 2726 | 2740 | Light grey to dull green, fine-grained rock with minute feldspar porphyrites. Feldspar replaced by clays. Moderately altered to green clays. Epidote noted. Flow-textured rock. Micro veins observed. | Trachyte | Illite, chlorite, epidote |
| 2740 | 2756 | Light green, subhedral, with poorly formed plagioclase (?) crystals. Medium- to fine-grained rock. Moderately altered and mafics present. | Basalt | Illite, chlorite, epidote, pyrite |
| 2758 | 2862 | Mixed cuttings of basaltic and grey trachytic fragments. Trachytic fragments are medium grained. Feldspar rich rock. Poorly altered and mafics noted in the rock. | Trachyte | Illite, chlorite, epidote |
| 2862 | 2892 | Earth grey, medium- to fine-grained rock, massive, with sanidine crystals being replaced by epidote and clays. Moderately altered, vein filling by epidote and mafics. | Trachytic intrusion | Epidote, actinolite, illite, pyrite |
| 2892 | 2900 | White, equigranular, medium-grained, felsic, silica and feldspar rich rock, with mafic specs. Shiny, golden brown illite noted on the groundmass. Secondary quartz growth observed. | Syenite | Epidote, illite, chlorite |
| 2900 | 2910 | Green to grey, medium-grained, massive rock with poorly formed/subhedral feldspar and quartz crystals. Volcanic glass also appears from the matrix. Mafics are being replaced by green clays. Micro veins also noted. | Rhyolite | Epidote, illite |
| 2910 | 2934 | Dull grey, fine grained, with sanidine crystals being replaced by clays. Alteration is moderate to high. Mafics also partially to fully replaced by clays. Micro veins also noted infilled with mafics/ferromagnesians? | Trachytic tuff | Illite, epidote, siderite |
| 2934 | 2988 | Light grey, medium grained, with coarse sanidine crystals and mafix. Epidote is replacing feldspars. Slight oxidation and minor sphene noted. | Trachyte | Illite, epidote, sphene |

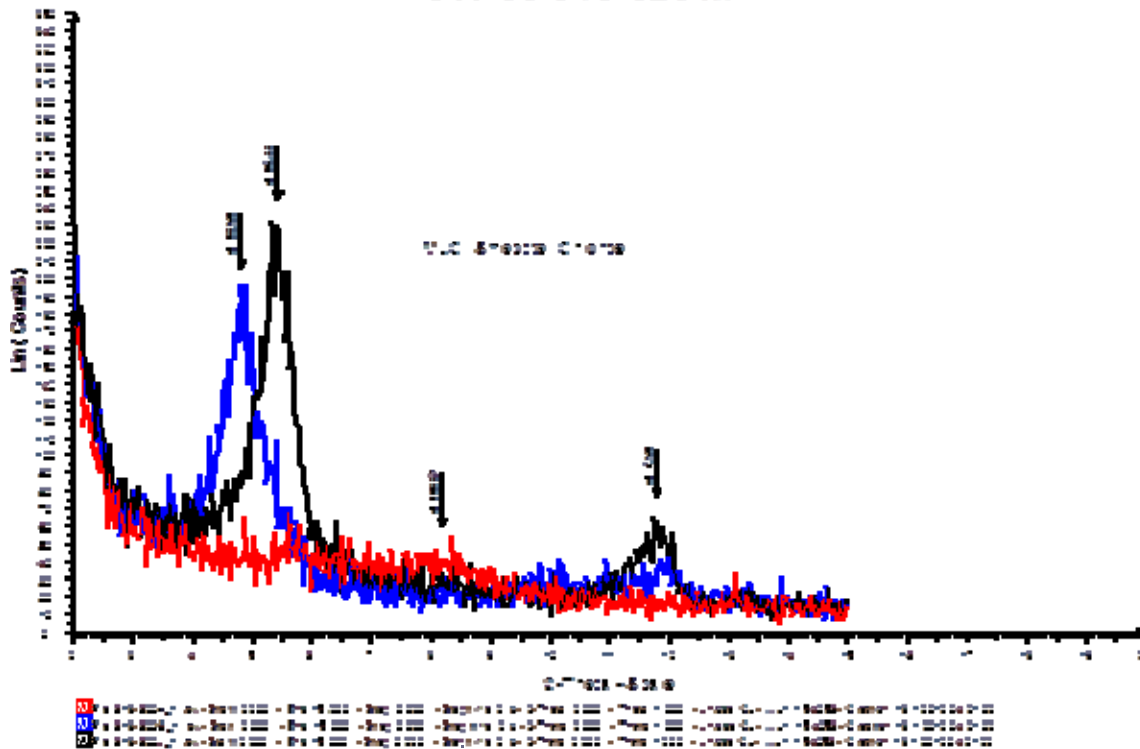**APPENDIX II: XRD graph analyses of chlorite, illite and mixed-layer clay peaks**

| Depth (m) | d(001) A | d(001) G | d(001) H | d(002) | Mineral |
|---|---|---|---|---|---|
| 38-40 | 14.78 | 19.58 | 10.5 | | Smectite |
| 58-60 | | | | | No clay. |
| 98-100 | | | | | No clay. |
| 138-140 | 15.49 | 18.37 | 10.56 | | Smectite |
| 178-180 | 11.04 | | | | Not confirmed. |
| 198-200 | 10.57 | 10.57 | 10.57 | | Illite |
| 218-220 | 10.84 | 10.84 | 10.84 | | Illite |
| 238-240 | 10.63 | 10.63 | 10.63 | | Illite |
| 258-260 | 10.56/8.79 | 10.56/8.79 | 10.56/8.79 | | Illite, amphibole |
| 278-280 | 10.93 | 10.93 | 10.93 | | Illite |
| 298-300 | | | | | No clay |
| 318-320 | 8.88 | 8.88 | 8.88 | | Amphibole |
| 338-340 | 8.88 | 8.88 | 8.88 | | Amphibole |
| 358-360 | | | | | No clay |
| 378-380 | 18.01 | 15.94 | 10.98 | 7.41, H=0 | Smectite, chlorite |
| 398-400 | 15.71 | 15.71 | 15.71 | 7.41, H=0 | Smectite, traces of chlorite |
| 418-420 | 16.33 | 18.50 | 10.55 | | Smectite |
| 438-440 | 15.94 | 18.50 | 10.98 | 7.38, H=0 | Smectite, chlorite |
| 458-460 | 16.13/8.96 | 18.50/8.96 | 12/8.96 | | Smectite, amphibole |
| 478-480 | 16.04 | 18.63 | 10.96 | 7.36, H=0 | Smectite, chlorite |
| 498-500 | 15.80 | 18.07 | | 7.45, H=0 | Smectite, chlorite (MLC) |
| 518-520 | 16.04 | 16.04 | 16.04 | 7.38, H=0 | Smectite, chlorite (MLC) |
| 538-540 | 16.47/8.64 | 18.01/8.64 | 10.67/8.64 | 7.61, H=0 | Smectite, chlorite (MLC) |
| 558-560 | 16.23 | 18.37 | 14.01 | 7.36, H=0 | Smectite, chlorite (MLC) |
| 598-600 | 13.29/10.74 | 13.29/10.74 | 13.29/10.74 | 7.36, H=0 | Chlorite, illite |
| 618-620 | 16.33 | 18.50 | 10.82 | 7.50, H=0 | Smectite, chlorite (MLC) |
| 638-640 | 15.14 | 18.56 | 12.29 | 7.33, H=0 | Smectite, chlorite (MLC) |
| 678-680 | 15.44/10.55 | 15.44/10.55 | 15.44/10.55 | 7.33, H=0 | Chlorite, illite |
| 698-700 | 15.62 | 15.62 | 15.62 | 7.34, H=0 | Chlorite |
| 718-720 | 15.94 | 15.94 | 15.94 | 7.26, H=0 | Chlorite |
| 738-740 | 16.28/10.70 | 16.28/10.70 | 16.28/10.70 | 7.34, H=0 | Chlorite, illite |
| 758-760 | 16.28/10.39 | 16.28/10.39 | 16.28/10.39 | 7.28, H=0 | Chlorite, illite |
| 778-780 | 15.44-12.46 /10.58 | 15.44-12.46/ 10.58 | 15.44-12.46/ 10.58 | 7.31, H=0 | Chlorite, illite |
| 818-820 | 15.09/10.64 | 15.09/10.64 | 15.09/10.64 | 7.28, H=0 | Chlorite, illite |
| 836-840 | 12.58 | 12.58 | 12.58 | 7.29, H=0 | Chlorite |
| 858-860 | 15.44 | 15.44 | 15.44 | 7.29, H=0 | Chlorite |
| 878-880 | 12.53 | 12.53 | 12.53 | | Chlorite |
| 898-900 | 15.44 | 15.44 | 15.44 | 7.40, H=0 | Chlorite |
| 918-920 | 12.43 | 12.43 | 12.43 | 7.29, H=0 | Chlorite |
| 938-940 | 13.96 | 13.96 | 13.96 | 7.37, H=0 | Chlorite |
| 978-980 | 15.31/10.80/ 8.90 | 15.31/10.80/ 8.90 | 15.31/10.80/ 8.90 | 7.46, H=0 | Chlorite, Illite, amphibole |
| 998-1000 | 14.88 | 14.88 | 14.88 | 7.31, H=0 | Chlorite |
| 1018-1020 | 10.61 | 10.61 | 10.61 | | Illite |
| 1078-1080 | 10.83 | 10.83 | 10.83 | 7.32, H=0 | Chlorite, illite |
| 1098-1100 | 10.58 | 10.58 | 10.58 | 7.34, H=0 | Chlorite, illite |
| 1138-1140 | 15.32 | 15.32 | 15.32 | 7.40, H=0 | Chlorite |
| 1158-1160 | 10.6 | 10.6 | 10.6 | 7.31, H=0 | Chlorite, illite |
| 1178-1180 | 10.8 | 10.8 | 10.8 | 7.33, H=0 | Chlorite, illite |
| 1198-1200 | 14.36/10.20 | 14.36/10.20 | 14.36/10.20 | 7.15, H=0 | Chlorite, illite |

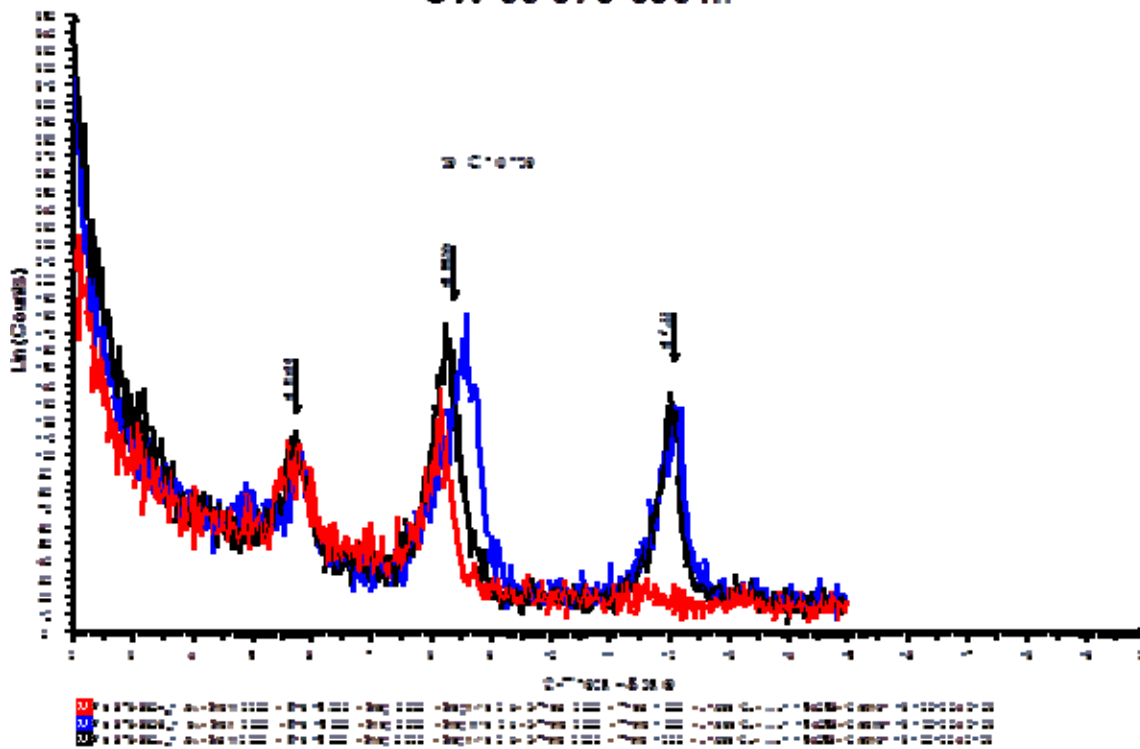| Depth (m) | d(001) A | d(001) G | d(001) H | d(002) | Mineral |
|---|---|---|---|---|---|
| 1218-1220 | 15.40/10.49 | 15.40/10.49 | 15.40/10.49 | 7.28, H=0 | Chlorite, illite |
| 1238-1240 | 15.40/10.49 | 15.40/10.49 | 15.40/10.49 | 7.28 | Chlorite, illite |
| 1258-1260 | 15.40/10.49 | 15.40/10.49 | 15.40/10.49 | 7.37, H=0 | Chlorite, illite |
| 1278-1280 | 15.32/10.68 | 15.32/10.68 | 15.32/10.68 | 7.37, H=0 | Chlorite, illite |
| 1298-1300 | 14.93/13.09/ 10.64/8.73 | 14.93/13.09/ 10.64/8.73 | 14.93/13.09/ 10.64/8.73 | | Chlorite, Illite, amphibole |
| 1318-1320 | 15.16/10.57 | 15.16/10.57 | 15.16/10.57 | 7.33, H=0 | Chlorite, illite |
| 1338-1340 | 15.16/10.60/ 6.56 | 15.16/10.60/ 6.56 | 15.16/10.60/ 6.56 | 7.31, H=0 | Chlorite, illite |
| 1358-1360 | 15.16/9.97 | 15.16/9.97 | 15.16/9.97 | 7.32, H=0 | Chlorite, illite |
| 1378-1380 | 14.83/10.40 | 14.83/10.40 | 14.83/10.40 | 7.29, H=0 | Chlorite, illite |
| 1418-1420 | 12.70/10.67 | 12.70/10.67 | 12.70/10.67 | 7.32, H=0 | Chlorite, illite |
| 1458-1460 | 12.56 | 12.56 | 12.56 | 7.38, H=0 | Chlorite |
| 1476-1478 | 13.13/10.67 | 13.13/10.67 | 13.13/10.67 | 7.38, H=0 | Chlorite, illite |
| 1498-1500 | 13.13/10.64 | 13.13/10.64 | 13.13/10.64 | 7.42, H=0 | Chlorite, illite |
| 1518-1520 | 12.62/10.56 | 12.62/10.56 | 12.62/10.56 | 7.40, H=0 | Chlorite, illite |
| 1538-1540 | 15.58/10.43 | 15.58/10.43 | 15.58/10.43 | 7.36, H=0 | Chlorite, illite |
| 1558-1560 | 15.58/10.43 | 15.58/10.43 | 15.58/10.43 | 7.35, H=0 | Chlorite, illite |
| 1578-1580 | 14.77 | 14.77 | 14.77 | 7.35, H=0 | Chlorite |
| 1598-1600 | 15.27/10.48 | 15.27/10.48 | 15.27/10.48 | 7.33, H=0 | Chlorite, illite |
| 1618-1620 | 10.57 | 10.57 | 10.57 | 7.31, H=0 | Illite, prob. chlorite |
| 1638-1640 | 15.21/10.57/ 8.84 | 15.21/10.57/ 8.84 | 15.21/10.57/ 8.84 | 7.33, H=0 | Chlorite, illite, amphibole |
| 1698-1700 | 12.62/10.54 | 12.62/10.54 | 12.62/10.54 | 7.31, H=0 | Chlorite, illite |
| 1738-1740 | 15.50/10.76 | 15.50/10.76 | 15.50/10.76 | 7.33, H=0 | Chlorite, illite |
| 1758-1760 | 13.12/10.69 | 13.12/10.69 | 13.12/10.69 | 7.38, H=0 | Chlorite, illite |
| 1798-1800 | 13.05/10.69 | 13.05/10.69 | 13.05/10.69 | 7.37, H=0 | Chlorite, illite |
| 1818-1820 | 14.78/10.40 | 14.78/10.40 | 14.78/10.40 | 7.24, H=0 | Chlorite, illite |
| 1838-1840 | 12.93/10.88 | 12.93/10.88 | 12.93/10.88 | 7.45, H=0 | Chlorite, illite |
| 1878-1880 | 12.93/10.62 | 12.93/10.62 | 12.93/10.62 | 7.33, H=0 | Chlorite, illite |
| 1898-1900 | 12.99/10.66 | 12.99/10.66 | 12.99/10.66 | 7.35, H=0 | Chlorite, illite |
| 1958-1960 | 12.93/10.66 | 12.93/10.66 | 12.93/10.66 | 7.38, H=0 | Chlorite, illite |
| 1978-1980 | 12.74/10.62 | 12.74/10.62 | 12.74/10.62 | 7.34, H=0 | Chlorite, illite |
| 1998-2000 | 13.06/10.76 | 13.06/10.76 | 13.06/10.76 | 7.42, H= 0 | Chlorite, illite |
| 2018-2020 | 12.94/10.62 | 12.94/10.62 | 12.94/10.62 | 7.34, H= 0 | Chlorite, illite |
| 2038-2040 | 15.33/10.72 | 15.33/10.72 | 15.33/10.72 | 7.31, H= 0 | Chlorite, illite |
| 2058-2060 | 15.33/10.72 | 15.33/10.72 | 15.33/10.72 | 7.31, H= 0 | Chlorite, illite |
| 2238-2240 | 10.66/8.84 | 10.66/8.84 | 10.66/8.84 | 7.36, H= 0 | Illite, amphibole, prob. chlorite |
| 2258-2260 | 15.14/10.57/ 8.76 | 15.14/10.57/ 8.76 | 15.14/10.57/ 8.76 | 7.36, H= 0 | Chlorite, Illite, amphibole |
| 2278-2280 | 13.22/10.66 | 13.22/10.66 | 13.22/10.66 | 7.75, H= 0 | Chlorite, illite |
| 2298-2300 | 13.20/10.61 | 13.20/10.61 | 13.20/10.61 | 7.75, H= 0 | Chlorite, illite |
| 2318-2320 | 12.88/10.62/ 8.86 | 12.88/10.62/ 8.86 | 12.88/10.62/ 8.86 | 7.75, H= 0 | Chlorite, Illite, amphibole |
| 2338-2340 | 13.03/10.62/ 8.79 | 13.03/10.62/ 8.79 | 13.03/10.62/ 8.79 | 7.38, H=0 | Chlorite, Illite, amphibole |
| 2358-2360 | 10.74/8.88 | 10.74/8.88 | 10.74/8.88 | | Illite, amphibole |
| 2378-2380 | 10.56 | 10.56 | 10.56 | 7.33, H =0 | Illite, prob. chlorite |
| 2398-2400 | 10.56 | 10.56 | 10.56 | 7.38, H=0 | Illite, prob. chlorite |
| 2418-2420 | 10.76/8.81 | 10.76/8.81 | 10.76/8.81 | 7.33, H =0 | Illite, prob. chlorite, amphibole |
| 2438-2440 | 15.44/10.63 | 15.44/10.63 | 15.44/10.63 | 7.32, H=0 | Illite, chlorite |
| 2498-2500 | 15.44/10.65/ 8.81 | 15.44/10.65/ 8.81 | 15.44/10.65/ 8.81 | 7.37, H= 0 | Illite, chlorite, amphibole |

| Depth (m) | d(001) A | d(001) G | d(001) H | d(002) | Mineral |
|---|---|---|---|---|---|
| 2518-2520 | 10.71 | 10.71 | 10.71 | 7.35, H= 0 | Illite, prob. chlorite |
| 2558-2560 | 15.61/10.71/ 8.81 | 15.61/10.71/ 8.81 | 15.61/10.71/ 8.81 | 7.33, H =0 | Illite, chlorite,  amphibole |
| 2578-2580 | 10.71 | 10.71 | 10.71 | 7.33, H =0 | Illite, prob. chlorite |
| 2598-2600 | 10.66 | 10.66 | 10.66 | | Illite |
| 2618-2620 | 10.49 | 10.49 | 10.49 | | Illite |
| 2698-2700 | 10.72 | 10.72 | 10.72 | | Illite |
| 2718-2720 | 14.92/10.51 | 14.92/10.51 | 14.92/10.51 | 7.29, H =0 | Illite, chlorite |
| 2758-2760 | 14.92/10.51 | 14.92/10.51 | 14.92/10.51 | 7.29, H =0 | Illite, chlorite |
| 2778-2780 | 14.92/10.65 | 14.92/10.65 | 14.92/10.65 | 7.36, H= 0 | Illite, chlorite, |
| 2798-2800 | 10.63 | 10.63 | 10.63 | | Illite |
| 2818-2820 | 10.74/8.83 | 10.74/8.83 | 10.74/8.83 | 7.35, H= 0 | Illite, amphibole, prob. chlorite |
| 2858-2860 | 10.63/8.83 | 10.63/8.83 | 10.63/8.83 | | Illite, amphibole |
| 2898-2900 | 10.55/8.76 | 10.55/8.76 | 10.55/8.76 | 7.31, H= 0 | Illite, amphibole, prob. chlorite |
| 2938-2940 | 10.58/8.76 | 10.58/8.76 | 10.58/8.76 | | Illite, amphibole |
| 2958-2960 | 10.78/8.85 | 10.78/8.85 | 10.78/8.85 | | Illite, amphibole |

**APPENDIX III: Selected XRD interpreted graphs for OW-35**



OW 35 398-400 m

## OW 35 418-420 m



## OW 35 618-620 m

## OW 35 678-680 m



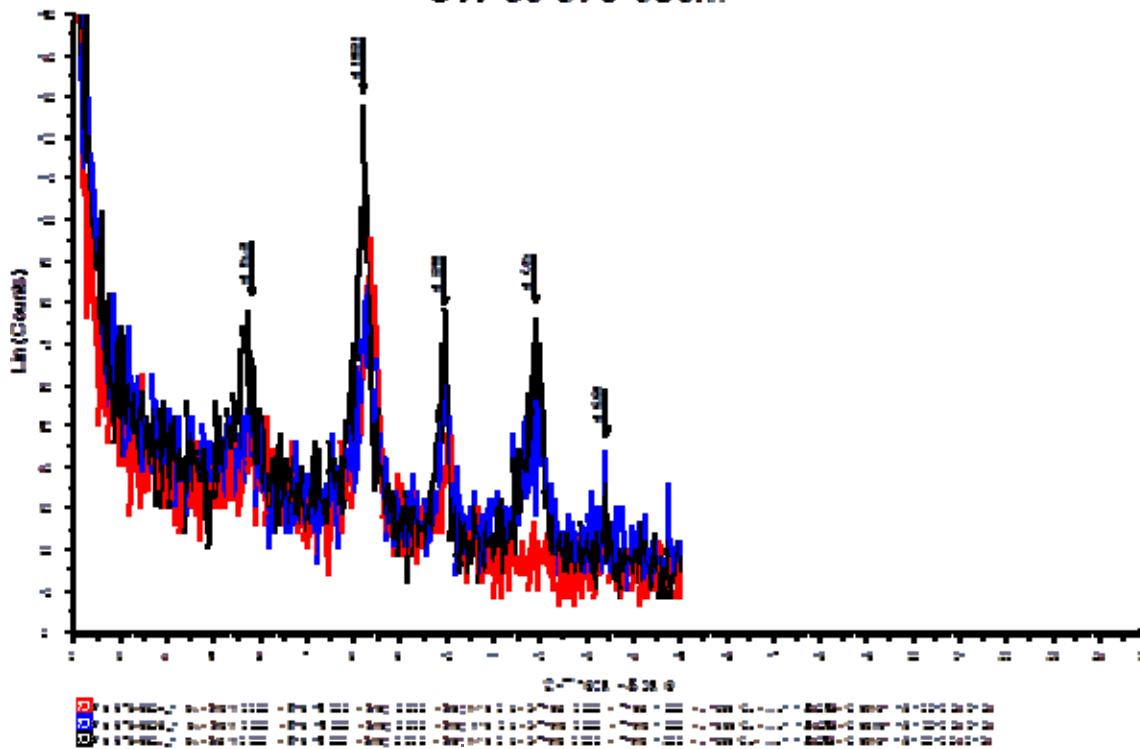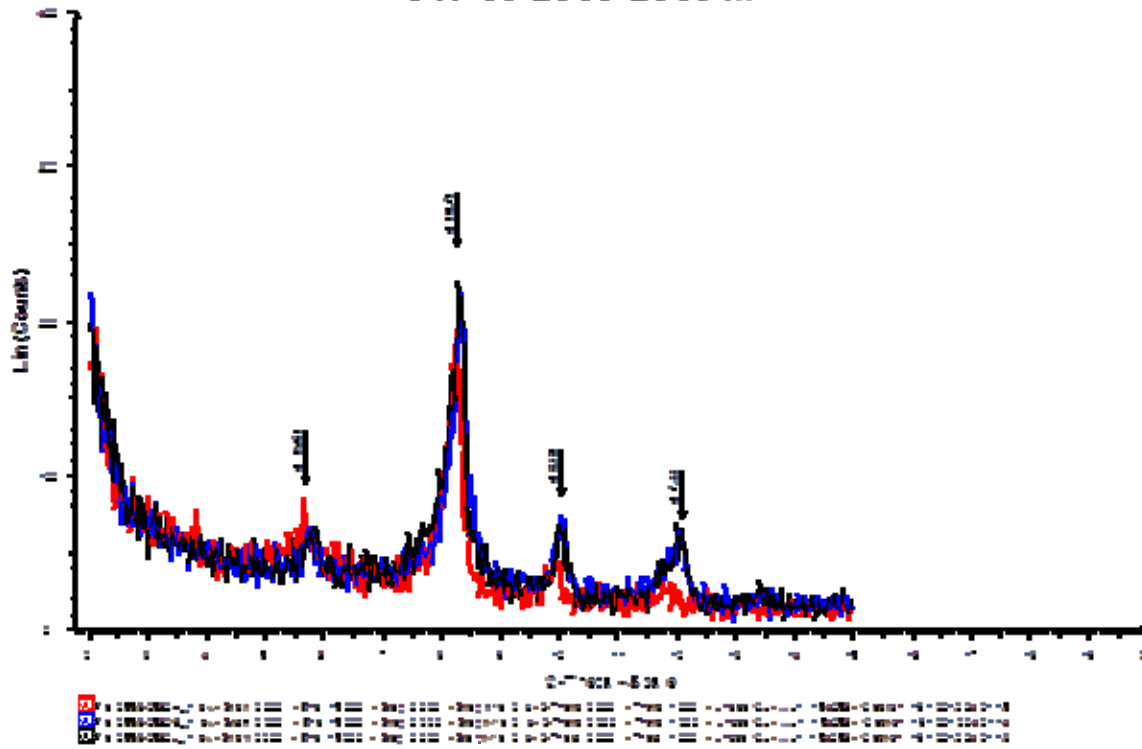## OW 35 978-980m

## OW 35 2558-2560 m



## OW 35 2818-2820 m